

2-15-2011

A Complexity-Reduced H-Matrix Based Direct Integral Equation Solver with Prescribed Accuracy for Large-Scale Electrodynamic Analysis

Wenwen Chai

Electrical and Computer Engineering, Purdue University, wchai@purdue.edu

Dan Jiao

Purdue University - Main Campus Electrical and Computer Engineering, Purdue University, djiao@purdue.edu

Follow this and additional works at: <http://docs.lib.purdue.edu/ecetr>

Chai, Wenwen and Jiao, Dan, "A Complexity-Reduced H-Matrix Based Direct Integral Equation Solver with Prescribed Accuracy for Large-Scale Electrodynamic Analysis" (2011). *ECE Technical Reports*. Paper 411.
<http://docs.lib.purdue.edu/ecetr/411>

This document has been made available through Purdue e-Pubs, a service of the Purdue University Libraries. Please contact epubs@purdue.edu for additional information.

A Complexity-Reduced \mathcal{H} -Matrix Based Direct
Integral Equation Solver with Prescribed Accuracy
for Large-Scale Electrodynamic Analysis

Wenwen Chai

Dan Jiao

TR-ECE-11-04

February 15, 2011

School of Electrical and Computer Engineering

1285 Electrical Engineering Building

Purdue University

West Lafayette, IN 47907-1285

A Complexity-Reduced \mathcal{H} -Matrix Based Direct
Integral Equation Solver with Prescribed Accuracy
for Large-Scale Electrodynamic Analysis

Wenwen Chai and Dan Jiao

School of Electrical and Computer Engineering
465 Northwestern Ave.
Purdue University
West Lafayette, IN 47907-2035

Abstract

In this paper, we develop an \mathcal{H} -matrix-based fast direct integral equation solver that has a significantly reduced computational complexity, with prescribed accuracy satisfied, to solve large-scale electrodynamic problems. In light of the fact that the cost of an \mathcal{H} -matrix-based computation of high-frequency problems is not only determined by the block rank that increases with electric size, but also determined by the \mathcal{H} -matrix partition, we propose a new parameter, average *partition* rank k_{ave} , to derive the storage units and operation counts of the \mathcal{H} -matrix based computation of electrodynamic problems. Different from block rank, the *partition* rank k_{ave} contains the information of the \mathcal{H} -matrix partition. We show that the computational cost of an \mathcal{H} -matrix-based computation of electrodynamic problems can be significantly reduced without sacrificing accuracy, by minimizing the rank of each admissible block based on accuracy requirements; and by optimizing the \mathcal{H} -partition to reduce the number of admissible blocks at each tree level for a prescribed accuracy and for each frequency point. To minimize the rank for a given accuracy, we develop an efficient matrix algebra based method to determine the minimal rank for each admissible block. The algebraic method has a linear complexity, and hence the computational overhead is negligible. To minimize the number of admissible blocks at each tree level for a given accuracy, we develop a new \mathcal{H} -partition method that is frequency dependent, and also controlled by accuracy requirements. With the proposed cost reduction methods, we develop a fast LU factorization for directly solving the dense system matrix resulting from an IE-based analysis of large-scale electrodynamic problems. The proposed solver successfully factorizes dense matrices that involve more than 1 million unknowns associated with electrodynamic problems of 96 wavelengths in fast CPU time, modest memory consumption, and with the prescribed accuracy satisfied. As an algebraic method, the underlying fast technique is kernel independent.

A Complexity-Reduced \mathcal{H} -Matrix Based Direct Integral Equation Solver with Prescribed Accuracy for Large-Scale Electrodynamic Analysis

Wenwen Chai, and Dan Jiao, *Senior Member, IEEE*

Abstract—In this paper, we develop an \mathcal{H} -matrix-based fast direct integral equation solver that has a significantly reduced computational complexity, with prescribed accuracy satisfied, to solve large-scale electrodynamic problems. In light of the fact that the cost of an \mathcal{H} -matrix-based computation of high-frequency problems is not only determined by the block rank that increases with electric size, but also determined by the \mathcal{H} -matrix partition, we propose a new parameter, average *partition* rank k_{ave} , to derive the storage units and operation counts of the \mathcal{H} -matrix-based computation of electrodynamic problems. Different from block rank, the *partition* rank k_{ave} contains the information of the \mathcal{H} -matrix partition. We show that the computational cost of an \mathcal{H} -matrix-based computation of electrodynamic problems can be significantly reduced without sacrificing accuracy, by minimizing the rank of each admissible block based on accuracy requirements; and by optimizing the \mathcal{H} -partition to reduce the number of admissible blocks at each tree level for a prescribed accuracy and for each frequency point. To minimize the rank for a given accuracy, we develop an efficient matrix algebra based method to determine the minimal rank for each admissible block. The algebraic method has a linear complexity, and hence the computational overhead is negligible. To minimize the number of admissible blocks at each tree level for a given accuracy, we develop a new \mathcal{H} -partition method that is frequency dependent, and also controlled by accuracy requirements. With the proposed cost reduction methods, we develop a fast LU factorization for directly solving the dense system matrix resulting from an IE-based analysis of large-scale electrodynamic problems. The proposed solver successfully factorizes dense matrices that involve more than 1 million unknowns associated with electrodynamic problems of 96 wavelengths in fast CPU time, modest memory consumption, and with the prescribed accuracy satisfied. As an algebraic method, the underlying fast technique is kernel independent.

Index Terms—Integral-equation-based methods, electromagnetic analysis, direct solution, \mathcal{H} matrix, large-scale analysis

I. INTRODUCTION

The Integral equation (IE) based computational electromagnetic methods generally lead to dense systems of linear equations. When a direct method is used, the operation count is proportional to $O(N^3)$ and the memory requirement is proportional to $O(N^2)$, with N being the matrix size. When an iterative solver is used, the memory requirement remains the same, and the computing time is proportional to $O(N_{it}N^2)$, where N_{it} denotes the total number of iterations required to

reach convergence. In recent years, fast solvers such as fast multipole based methods [1]–[3], fast low-rank compression methods [4]–[7], and FFT-based methods [8], [9] have been developed that dramatically reduce the memory requirement of the iterative IE solvers to $O(N)$, and the CPU time to $O(N_{it}N \log N)$ for electrodynamic problems. This represents an impressive improvement as compared with conventional $O(N^3)$ or $O(N_{it}N^2)$ techniques.

Fast direct solvers have also been developed for electrodynamic problems. Most recent work can be seen in [10], [11]. LU factorization of $O(N^2)$ time complexity and $O(N^{1.5})$ memory complexity has been reported. Compared to iterative solvers, direct solvers have advantages when the number of iterations is large or the number of right hand sides is large. For example, if there exist N right hand sides, each of which costs $O(N_{it}N \log N)$ operations, the total cost of the iterative solver will be $O(N_{it}N^2 \log N)$, which is expensive.

Recently, the \mathcal{H} - and \mathcal{H}^2 -matrix based mathematical framework has been introduced and further developed to reduce the computational complexity of iterative IE-based solvers for electrodynamic problems [12], [13]. It is shown that given a wide range of electric sizes which lead to a wide range of N , the dense system of $O(N^2)$ parameters can be compactly stored in $O(N)$ units, and the dense matrix-vector multiplication can be performed in $O(N)$ operations. Moreover, the same order of accuracy can be kept across this range.

In this work, under the mathematical framework of the \mathcal{H} matrix, we develop a fast direct IE solver that has a significantly reduced computational complexity, with the prescribed accuracy satisfied, to solve large-scale electrodynamic problems. The \mathcal{H} (hierarchical)-matrix is a general mathematical framework [14]–[17], which enables a highly compact representation and efficient numerical computation of dense matrices. To be specific, if matrix \mathbf{C} is an $m \times n$ off-diagonal block in an \mathcal{H} matrix that describes a far-field interaction specified by a so-called admissibility condition [17], it can be written as $\mathbf{C} = \mathbf{A}\mathbf{B}^T$, where \mathbf{A} is of dimension $m \times k$, \mathbf{B} is of dimension $n \times k$, and k denotes the rank of \mathbf{C} with $k < m$ and $k < n$. Storage requirements and matrix-vector multiplications using \mathcal{H} -matrices have been shown to be of complexity $O(N \log N)$. From a mathematical point of view, existing low-rank compression based IE methods developed for electromagnetic analysis can be viewed in the framework of \mathcal{H} matrices, although their technical details could be very different and many of them predated the literature of \mathcal{H} matri-

ces. For example, the direct integral equation solver reported in [10] can be viewed as an \mathcal{H} -based direct integral equation solver, although \mathcal{H} -based fast arithmetics was not employed. It successfully solves electrically large integral equations for problem sizes to 1 M unknowns. It is also worth mentioning that the matrices underlying generic Fast Multipole algorithms are \mathcal{H}^2 -matrices, as noted in [19].

In the literature of \mathcal{H} matrices, it is shown that matrix-matrix multiplications and matrix inversions using \mathcal{H} -matrices are of complexity $O(N \log^2 N)$ [14]–[17], which is very efficient. However, the actual complexity of an \mathcal{H} -matrix based method is associated with the rank k of the off-diagonal blocks. For static problems, a constant k can be used for all problem sizes without sacrificing accuracy, and hence ignored in complexity analysis. For electrodynamic problems, however, the k required to achieve a given accuracy typically increases with the electric size [12], [21]. Since the rank k becomes a variable in electrodynamic analysis, the existing complexity analysis developed for \mathcal{H} -matrix based arithmetics [17], which is based on a constant rank, becomes not proper for analyzing electrodynamic problems. To be specific, if one uses the maximum rank of all the admissible blocks to bound the complexity, the complexity is overestimated. More importantly, the complexity of an \mathcal{H} -matrix based computation of electrodynamic problems is highly dependent on the \mathcal{H} -matrix partition, i.e. the number of admissible blocks and the row/column dimension of each block etc. This is an important factor that received little attention in previous research. Existing \mathcal{H} -matrix partition is based on a geometry based admissibility condition. The resultant partition is by no means optimal especially for electrodynamic problems.

In this work, we develop new bounds of the computational cost for the \mathcal{H} -matrix-based computation of electrodynamic problems. In light of the fact that the complexity of an \mathcal{H} -matrix based computation of electrodynamic problems is determined by both block rank (the rank of each admissible block) and \mathcal{H} -matrix partition, we propose a new parameter, average partition rank k_{ave} , to bound the storage units and operation counts of an \mathcal{H} -matrix based computation. Different from block rank, the partition rank k_{ave} contains the information of the \mathcal{H} -matrix partition.

With the new bounds of the computational cost derived for electrodynamic problems, it becomes clear how to reduce the complexity of an \mathcal{H} -matrix based computation for solving high-frequency problems. We propose two methods. One is to minimize the rank of each admissible block based on accuracy requirements. Although the block rank is observed to be proportional to the electric size of the block diameter, the actual number should be determined and minimized based on accuracy requirements. We determine the minimal rank for each admissible block by an efficient matrix algebra based method. The algebraic method has a linear complexity, and hence the computational overhead is negligible. The other method for reducing the computational cost is to optimize the \mathcal{H} -partition to reduce the number of admissible blocks at each tree level based on accuracy requirements for each frequency point. We show that the admissibility condition used in the conventional \mathcal{H} -partition is empirical instead of

theoretical, and hence not optimal for a given accuracy and a given frequency. We hence develop a new \mathcal{H} -partition method that is frequency dependent, and also controlled by accuracy requirements. With the proposed new partition, the number of admissible blocks at each tree level is significantly reduced compared to that generated by the admissibility condition based, i.e. geometry based partition. The methods we developed for minimizing the rank and optimizing the \mathcal{H} -partition not only can be used in the proposed solver, but also can be used in other fast integral equation solvers to speed up their computation.

Moreover, we developed an efficient LU-factorization for directly solving the dense system matrix resulting from an IE-based analysis of large-scale electrodynamic problems. The operation counts of the proposed direct solver are $O((k_{ave}C_{sp})^2 N \log^2 N)$ in LU factorization, $O((k_{ave}C_{sp})N \log N)$ in LU solution, and the storage requirement is $O(k_{ave}C_{sp}N \log N)$, all of which were derived theoretically and also verified numerically. The C_{sp} is the maximal number of blocks that can be formed by a cluster in a block cluster tree. Although both k_{ave} and C_{sp} depend on N in electrodynamic analysis, that is why we include these two parameters in the computational cost, they are reduced to small numbers compared to N by the proposed methods. We also give a detailed implementation of the \mathcal{H} -based LU factorization, which is not reported elsewhere.

The remainder of this paper is organized as follows. In Section II, we give the background of the \mathcal{H} -matrix based analysis of electrodynamic problems. In Section III, we propose the new bounds of the computational cost for the \mathcal{H} -matrix based computation of electrodynamic problems. In Section IV, we propose methods to reduce the complexity of the \mathcal{H} -matrix based computation. In Section V, we give a numerical proof on the existence of an \mathcal{H} -matrix based representation of the inverse and LU factors of an IE based system matrix for an electrodynamic problem. In Section VI, we give a number of pseudo-codes to show a detailed implementation of the LU factorization using \mathcal{H} matrices, which is not reported in the mathematical literature. In Section VII, we analyze computational cost. In Section VIII, we present numerical results to demonstrate the accuracy and efficiency of the proposed direct IE solver. In Section IX, we summarize our findings.

II. BACKGROUND

The \mathcal{H} -matrix based methods are kernel independent. In the following, we use an electric-field integral equation as an example to illustrate the basic concept of \mathcal{H} -matrix based methods.

A. Electric Field Integral Equation

We consider the electric-field integral equation (EFIE) [1], [22]

$$\mathbf{E}_i|_{tan} = \iint_S [j\omega\mu\mathbf{J}_S(\mathbf{r})g(\mathbf{r},\mathbf{r}')]|_{tan} dS' - \iint_S \left[\frac{j}{\omega\epsilon} (\nabla' \cdot \mathbf{J}_S(\mathbf{r}')) \nabla' g(\mathbf{r},\mathbf{r}') \right]_{tan} dS', \quad (1)$$

in which Green's function $g(\mathbf{r}, \mathbf{r}') = \frac{e^{-j\kappa|\mathbf{r}-\mathbf{r}'|}}{|\mathbf{r}-\mathbf{r}'|}$, \mathbf{J}_S is the induced surface current density, ω is angular frequency, κ is wave number, and subscript *tan* denotes tangential component.

By expanding the unknown \mathbf{J}_S using the RWG basis functions [22], a Method of Moment based solution of (1) results in the following linear system of equations

$$\mathbf{G}\mathbf{I} = \mathbf{V}, \quad (2)$$

where

$$\mathbf{G}_{mn} = \iint_{S_m} dS \iint_{S_n} dS' [j\omega\mu\mathbf{J}_m(\mathbf{r}) \cdot \mathbf{J}_n(\mathbf{r}') - \frac{j}{\omega\epsilon} (\nabla \cdot \mathbf{J}_m(\mathbf{r})) (\nabla' \cdot \mathbf{J}_n(\mathbf{r}'))] g(\mathbf{r}, \mathbf{r}'), \quad (3)$$

and

$$V_m = \iint_{S_m} \mathbf{J}_m(\mathbf{r}) \cdot \mathbf{E}_i dS. \quad (4)$$

The conventional way to solve (2) could be very expensive, since the entries of \mathbf{G} are all nonzero. In the following section, we introduce the \mathcal{H} matrix as a data-sparse representation of \mathbf{G} , from which a significant reduction in computational complexity can be achieved.

B. Definition of the \mathcal{H} Matrix

An \mathcal{H} matrix is generally associated with an admissibility condition [17]. To define an admissibility condition, we denote the whole index set containing the indices of the basis functions in the computational domain by $\mathcal{I} = \{1, 2, \dots, N\}$, where N is the total number of unknowns. Considering two subsets t and s of the \mathcal{I} , the admissibility condition is defined as

$$(t, s) \text{ are admissible} = \begin{cases} \text{True} & \text{if } \min\{\text{diam}(Q_t), \text{diam}(Q_s)\} \\ & \leq \eta \text{dist}(Q_t, Q_s); \\ \text{False} & \text{otherwise,} \end{cases} \quad (5)$$

where, as shown in Fig. 1, $Q_{t,s}$ is the minimal subset of the space containing the supports of all basis functions belonging to t or s , $\text{diam}(\cdot)$ is the Euclidean diameter of a set, $\text{dist}(\cdot)$ is the Euclidean distance of two sets, and η is a positive parameter that can be used to control the admissibility condition. If subsets t and s do not satisfy the admissibility condition, they are called inadmissible. The admissibility condition shown in (5) is rather empirical than theoretical. It is controlled by an empirical parameter η , instead of a prescribed accuracy. In this work, we will develop a new method to partition a matrix into admissible and inadmissible blocks, which is controlled by accuracy requirements.

In an \mathcal{H} -matrix representation, an inadmissible block keeps its original full-matrix representation; while an admissible block has a factorized low-rank form. To be specific, an admissible block $\mathbf{G}^{t,s}$ that is formed by subsets t and s can be written as a factorized form

$$\mathbf{G}^{t,s} = \mathbf{A}\mathbf{B}^T, \quad (6)$$

where $\mathbf{G}^{t,s} \in \mathbb{C}^{m \times n}$, $\mathbf{A} \in \mathbb{C}^{m \times k}$, $\mathbf{B} \in \mathbb{C}^{n \times k}$, and $k \in \mathbb{N}$ is the rank of $\mathbf{G}^{t,s}$. Here, as long as k is less than the minimum

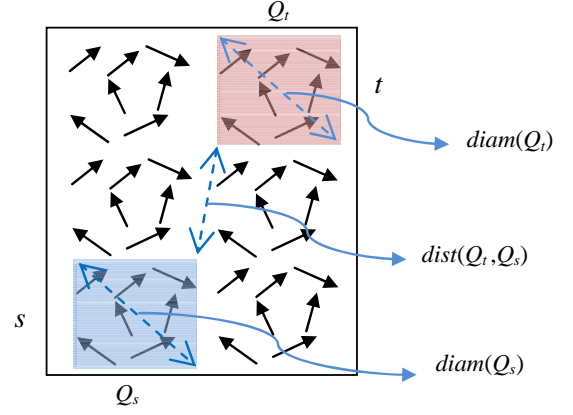


Fig. 1. An illustration of the admissibility condition.

of m and n , $\mathbf{G}^{t,s}$ is low rank. The k is not required to be $O(1)$.

If all the blocks $\mathbf{G}^{t,s}$ formed by the admissible (t, s) in \mathbf{G} can be represented by a factorized low-rank form shown in (6), \mathbf{G} has an \mathcal{H} -matrix representation ([17], p. 18). Clearly, to store admissible $\mathbf{G}^{t,s}$, we only need to store \mathbf{A} and \mathbf{B} , the cost of which is $O(k(m+n))$ in contrast with the original storage that is $O(mn)$. Similar cost reduction in matrix-vector and matrix-matrix multiplication can be achieved. Therefore, if we are able to represent the dense matrix resulting from an IE based analysis by an \mathcal{H} matrix, we can reduce the complexity of IE-based solutions significantly. The detail of the \mathcal{H} -matrix representation of an IE-based system matrix is given in next subsection.

C. \mathcal{H} -Matrix Representation of the IE-Based System Matrix

The essential idea of an \mathcal{H} -matrix representation is to represent the off-diagonal matrix block that satisfies the admissibility condition by a rank- k matrix shown in (6).

There are three representative schemes that can be used to generate a rank- k matrix of an IE-based dense matrix block: interpolation, Taylor expansion, and adaptive cross approximation (ACA). In [12], [13], an interpolation scheme is used to obtain an \mathcal{H} -representation without any compression cost for electrodynamic kernels. The error bound of the interpolation based \mathcal{H} -representation was derived. It was shown that exponential convergence with respect to the number of interpolation points can be achieved irrespective of the electric size. Taylor expansion can also be used to locally replace the kernel function by degenerate approximations, as shown in ([17], p. 10). Its accuracy is controlled by the expansion order. Neither interpolation nor Taylor expansion involves rank compression cost. Another approach is to directly compute a low rank approximation of the original matrix up to a prescribed accuracy. The representative method is ACA [17], [20], which is purely algebraic. In [10], [21], ACA was used to solve electromagnetic problems. For each matrix block, the cost of ACA is linear. A simple flow to obtain the \mathcal{H} -matrix representation of a given matrix block is shown in Fig. 2.

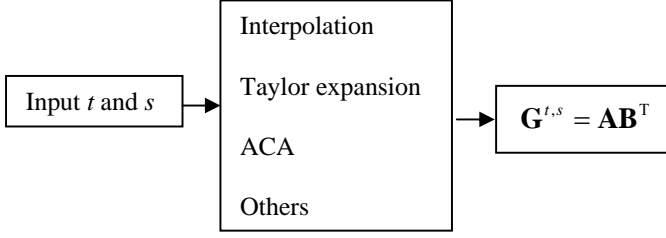


Fig. 2. A flow to obtain a rank- k matrix representation of a given dense matrix block.

D. \mathcal{H} -Matrix Partition

To use an \mathcal{H} -matrix representation, we have to partition a dense matrix into admissible blocks and inadmissible blocks. An admissible block is represented by a rank- k matrix shown in (6), and an inadmissible block is represented by a full-matrix form.

In [12], [13], we show how to build a cluster tree and a block cluster tree to efficiently carry out the \mathcal{H} -matrix partition for a dense matrix resulting from the IE-based analysis of electrodynamic problems. We denote the cluster tree constructed for the full index set \mathcal{I} by $T_{\mathcal{I}}$. We then find a disjoint partition of the index set and use this partition to create children clusters. We continue this procedure until the index number in each cluster is less than the *leafsize* which is a parameter to control the depth of the tree. A block cluster tree, as shown in Fig. 3(a), between cluster trees $T_{\mathcal{I}}$ and $T_{\mathcal{I}}$ is constructed based on a given admissibility condition recursively. In Fig. 3(a), each link in an upper level represents an admissible block shown by a shaded block in Fig. 3(b). The number of links is bounded by sparsity constant C_{sp} , which is the maximum number of blocks that can be formed by a cluster in a block cluster tree ([17], p. 125).

The admissible block cluster tree results in a matrix partition as shown in Fig. 3(b). The shaded matrix blocks are admissible blocks; the un-shaded ones are inadmissible blocks. The admissible blocks and inadmissible blocks together form a complete \mathcal{H} partition. In Fig. 3(b), we also label the levels present in an \mathcal{H} partition, which is shown by dashed rectangular boxes.

III. PROPOSED BOUNDS OF STORAGE UNITS AND OPERATION COUNTS FOR \mathcal{H} -MATRIX BASED COMPUTATION OF ELECTRODYNAMIC PROBLEMS

The complexity of \mathcal{H} -matrix based arithmetics has been conducted for kernel functions that do not change with frequencies [17]. Storage requirements and matrix-vector multiplications using \mathcal{H} -matrices have been shown to be of complexity $O(N \log N)$. Moreover, the inverse of an \mathcal{H} matrix can be obtained in $O(N \log^2 N)$ complexity. In this section, we show that for electrodynamic problems, the complexity bounds of \mathcal{H} -matrix based computations need to be re-derived. In light of the fact that the cost of an \mathcal{H} -matrix-based computation of high-frequency problems is not only determined by the block rank that increases with electric size, but also determined by the \mathcal{H} -partition, we propose a new parameter, average *partition*

rank k_{ave} , to bound the computational cost of the \mathcal{H} -matrix-based computation of electrodynamic problems. With the new bounds, it becomes clear how to reduce the complexity of an \mathcal{H} -matrix based computation for solving high-frequency problems.

A. Proposed definition of average partition rank, k_{ave} , for the \mathcal{H} -based computation of electrodynamic problems

For frequency independent kernels, a constant rank k across all the admissible blocks is sufficient to generate a constant order of accuracy for the \mathcal{H} -based computation of the dense system matrix. This can be theoretically verified from the error bound for an \mathcal{H} -matrix based representation of a static kernel [17]. For frequency dependent kernels, however, a constant k , in general, cannot guarantee a constant order of accuracy across a wide range of electric sizes. This can be seen from the error bound of an \mathcal{H} -matrix-based representation of electrodynamic problems [12], [13]. This can also be seen from ACA-based rank revealing presented in [21]. As a result, the complexity analysis of \mathcal{H} -based computations given in the mathematical literature, which is based on a constant rank, is not proper for analyzing electrodynamic problems.

Take the storage complexity of an \mathcal{H} -matrix as an example, which is also the complexity of an \mathcal{H} -matrix based matrix-vector multiplication. In an \mathcal{H} matrix, since each admissible block $\mathbf{G}^{m_i \times n_i}$ has a factorized form $\mathbf{A}_{m_i \times k_i} \mathbf{B}_{n_i \times k_i}^T$ with rank k_i , the storage is reduced from $m_i \times n_i$ units to $k_i(m_i + n_i)$ units. By summing up the storage of all the admissible blocks, we obtain

$$\text{Storage} = \sum_{i=1}^{nk} k_i(m_i + n_i), \quad (7)$$

where nk is the total number of admissible blocks. The above can be evaluated as

$$\text{Storage} = \sum_{l=0}^p \sum_{i=1}^{nk_l} k_i(m_i + n_i), \quad (8)$$

where l is tree level, p is tree depth, and nk_l is the number of admissible blocks at level l . Clearly, as can be seen from (7), if we use the maximal k among all the admissible blocks, k_{max} , to bound the computational complexity, we will overestimate the complexity because many admissible blocks have a rank much smaller than k_{max} . To give an example, in Fig. 4, we plot the storage of the blocks that have the largest rank k_{max} in comparison with that of the rest of the blocks that have a rank smaller than k_{max} , for a cone sphere across a wide range of electric sizes. The electric size ranges from $\kappa a = 2$ to $\kappa a = 600$, where κ is wave number and a is the largest physical dimension of the cone sphere. It is clear that the total storage is not dominated by the cost of storing rank- k_{max} blocks. In fact, the storage of the rank- k_{max} blocks is much less than that of the rest of the blocks. This is because although k_{max} is large, the number of admissible blocks that have rank k_{max} is also the smallest.

Furthermore, as can be seen from (8), in addition to the block rank k_i , the number of admissible blocks at each tree level nk_l also plays an important role in determining the

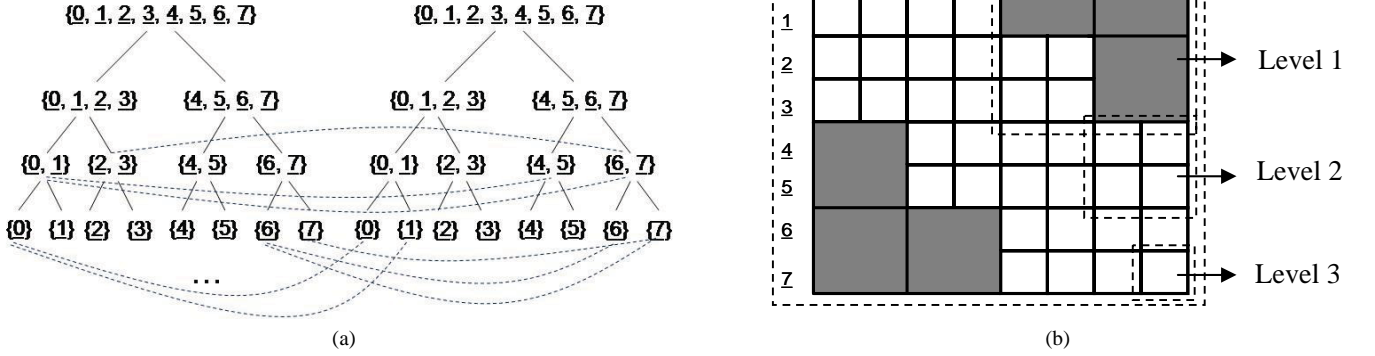


Fig. 3. (a) A block Cluster Tree. (b) An \mathcal{H} -matrix partition.

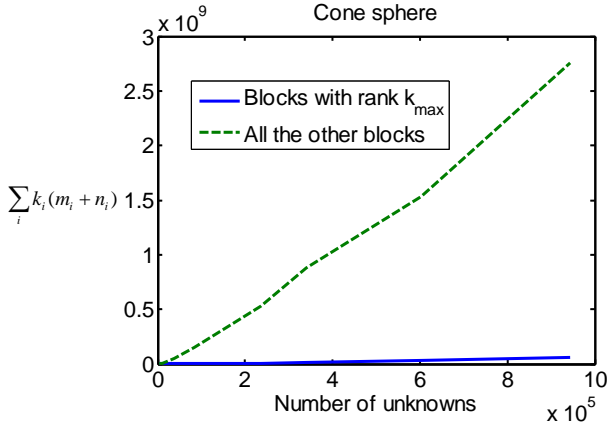


Fig. 4. Comparison between the storage of the rank- k_{max} blocks and that of the other blocks for a cone-sphere from $\kappa_a = 2$ to $\kappa_a = 600$.

computational complexity. If nk_l is proportional to 2^l , then the advantage of the \mathcal{H} -based computation of high-frequency problems may not be significant since the block rank k_i is observed to be proportional to the electric size of the block diameter. However, in reality, nk_l is not proportional to 2^l . This will become clear in the following subsections. In addition, there exists a big space to optimize the \mathcal{H} -partition to reduce nk_l without sacrificing accuracy.

From the aforementioned analysis, the complexity of an \mathcal{H} -based computation of high-frequency problems is determined by the block rank k_i as well as the number of admissible blocks at each tree level and the row/column dimension of each admissible block, i.e. \mathcal{H} -partition. In light of this fact, we propose a new parameter, average *partition* rank k_{ave} , to derive the computational cost of an \mathcal{H} -based computation of high-frequency problems. We define average *partition* rank k_{ave} as the following:

$$k_{ave} = \frac{\sum_{i=1}^{nk} k_i(m_i + n_i)}{\sum_{i=1}^{nk} (m_i + n_i)}, \quad (9)$$

where nk is the total number of admissible blocks, k_i is the rank of the i -th admissible block, m_i and n_i are the number of rows and columns of the admissible block. From the above

definition, it is clear that k_{ave} is not only related to the block rank k_i , but also related to the \mathcal{H} -partition. Different partitions can result in different k_{ave} . That is why we name k_{ave} as average *partition* rank to distinguish it from the *block* rank that does not contain any information about partition.

B. Proposed bounds of storage units and operation counts for the \mathcal{H} -based computation of electrodynamic problems

By using (9), the storage complexity (7) can be written as

$$\text{Storage} = k_{ave} \sum_{i=1}^{nk} (m_i + n_i), \quad (10)$$

The summation of the m_i and n_i over all the admissible blocks can be evaluated as the following:

$$\sum_{i=1}^{nk} (m_i + n_i) \leq \sum_{l=0}^p \sum_{i=1}^{nk_l} \left(\frac{N}{2^l} \times 2 \right) = \sum_{l=0}^p nk_l \left(\frac{N}{2^l} \times 2 \right), \quad (11)$$

in which we use the fact that the row/column dimension of a block at level l is $\frac{N}{2^l}$, where $l = 0$ represents the root level. The above should be evaluated based on actual nk_l , which is problem dependent and partition dependent. Here, we use the fact that nk_l is less than $2^l C_{sp}$ to bound (11), substituting (11) into (10), we thus obtain

$$\text{Storage} = O(k_{ave} C_{sp} N \log N). \quad (12)$$

Therefore, we can use the average *partition* rank defined in (9) to bound the storage units.

Similarly, we can use an average *square partition* rank defined below to bound the operation counts of the \mathcal{H} -based computation.

$$(k^2)_{ave} = \frac{\sum_{i=1}^{nk} k_i^2(m_i + n_i)}{\sum_{i=1}^{nk} (m_i + n_i)}. \quad (13)$$

Take the matrix-matrix multiplication as an example, the cost for each admissible block involved in the multiplication is $C_{sp} k_i^2(m_i + n_i)$ ([17], pp. 127-130). By summing up the cost of all the admissible blocks across all the tree levels, we

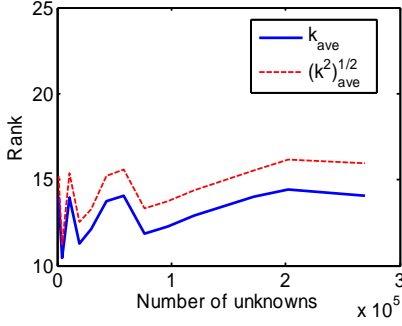


Fig. 5. Comparison of two average partition rank for a 3D PEC plate with electric size from 2 to 30 wavelengths.

obtain

$$\begin{aligned}
 \text{Operation counts} &= C_{sp} \sum_{l=0}^p \sum_{i=1}^{nk} k_i^2 (m_i + n_i) \\
 &\leq C_{sp} \sum_{l=0}^p (k^2)_{ave} \sum_{i=1}^{nk} (m_i + n_i) \quad (\text{From (13)}) \\
 &\leq C_{sp} (k^2)_{ave} \sum_{l=0}^p \sum_{i=1}^{nk} (m_i + n_i) \\
 &\leq C_{sp}^2 (k^2)_{ave} O(N \log^2 N),
 \end{aligned}
 \tag{14}$$

where p is the tree depth that is proportional to $\log N$. From (13) and (9), it can be seen that the $(k^2)_{ave}$ is an $O(k_{ave}^2)$ quantity. As an example, in Fig. 5, we plot k_{ave} and $\sqrt{(k^2)_{ave}}$ for a 3D conducting plate from 2 to 30 wavelengths. It can be seen that these two average rank follow each other closely. Therefore, we can also use k_{ave} to bound the CPU time cost of an \mathcal{H} -based computation of electrodynamic problems. We thus obtain

$$\text{Operation counts} \leq O((k_{ave} C_{sp})^2 N \log^2 N). \tag{15}$$

It is worth mentioning that the bounds derived above for storage and time cost are valid for any \mathcal{H} -partition. They are not specifically developed for the \mathcal{H} -partition based on the admissibility condition given in (5). Different partitions could result in different k_{ave} and C_{sp} . Moreover, different problems could have different k_{ave} and C_{sp} . However, regardless of the value of k_{ave} and C_{sp} , the storage units are bounded by (12), and the operation counts are bounded by (15). In addition, for electrodynamic problems, the k_{ave} and C_{sp} generally depend on N . The objective of this work is to minimize $k_{ave} C_{sp}$ based on accuracy requirements.

IV. PROPOSED METHODS FOR REDUCING THE COMPUTATIONAL COST OF \mathcal{H} -MATRIX BASED DIRECT SOLUTION OF ELECTRODYNAMIC PROBLEMS

From (12) and (15), it can be seen that to reduce the computational cost of an \mathcal{H} -based computation of electrodynamic problems, we have to reduce $k_{ave} C_{sp}$. In the following two subsections, we present methods for reducing $k_{ave} C_{sp}$.

A. Proposed methods for minimizing average partition rank k_{ave} based on a prescribed accuracy for a given \mathcal{H} -partition

Given an \mathcal{H} -partition, to minimize k_{ave} , for each admissible block, we determine a minimal rank based on a prescribed accuracy. The reason is obvious. If each admissible block has a minimal rank, the resultant average partition rank k_{ave} for the given \mathcal{H} partition is also minimized.

Given an accuracy requirement, singular value decomposition (SVD) is the most accurate method to obtain the minimum rank that can meet the accuracy requirement for an admissible block. However, if we directly apply SVD to the original full matrix to obtain its \mathcal{H} -matrix representation, although the resultant rank is minimal, the computational cost is high.

On the other hand, we can use interpolation, Taylor expansion, and ACA based approaches to efficiently convert a full matrix block to an \mathcal{H} -matrix representation. However, the resultant rank is, in general, not the minimal one that is necessary to satisfy the accuracy requirement. In other words, the resultant rank can be much larger than what is necessary to satisfy a prescribed accuracy.

In this paper, we first use ACA+ ([17], pp. 71-74), which is a variant of ACA, to efficiently compute an \mathcal{H} -matrix representation. We then apply SVD to the \mathcal{H} -matrix representation to determine the actual rank that is needed to satisfy the accuracy requirement. By doing so, we keep the advantages of both SVD and ACA-based methods. The resultant rank is minimal, and meanwhile it is obtained in linear complexity for each block. In the following, we give more details of the proposed approach.

First, we use ACA+ to numerically obtain a factorized form of an admissible block. Conventional ACA fails in some examples [20]. ACA+ does not have such a problem. In addition, ACA+ involves less storage and computational cost than ACA. The detailed procedure of ACA+ is very similar to that of the conventional ACA. The difference between them is as follows. At the beginning of an ACA+ algorithm, a reference row and a reference column of the original matrix are chosen to determine where to start the pivot search. A row and column pivot index is then determined from the reference ones. In the subsequent steps, the reference row and column can still be used. But if they are chosen as a pivot index, a new reference row and a new reference column has to be chosen. This method only requires assemble k rows and k columns of an admissible block, where k is the rank determined by a certain accuracy requirement ϵ . The output of ACA+ algorithm is $\mathbf{G}^{m,n} = \mathbf{A}_{m,k} \mathbf{B}_{n,k}^T$, where k is, in general, much less than m and n . The ACA+ algorithm terminates when

$$\|\mathbf{G} - \tilde{\mathbf{G}}\| = \|\mathbf{G} - \mathbf{A}\mathbf{B}^T\| \leq \epsilon \|\mathbf{G}\| \tag{16}$$

is satisfied. Therefore, the error of the resultant \mathcal{H} -matrix representation is bounded by ϵ .

After the ACA+ is completed, we obtain a factorized form $\mathbf{A}_{m,k} \mathbf{B}_{n,k}^T$. For such a factorized form, SVD can be efficiently performed by a reduced SVD ([17], p. 108). The resultant computational cost is $O(k^2(m+n))$, which is linear.

To test the effectiveness of the proposed approach to determining the minimal rank of an admissible block, we

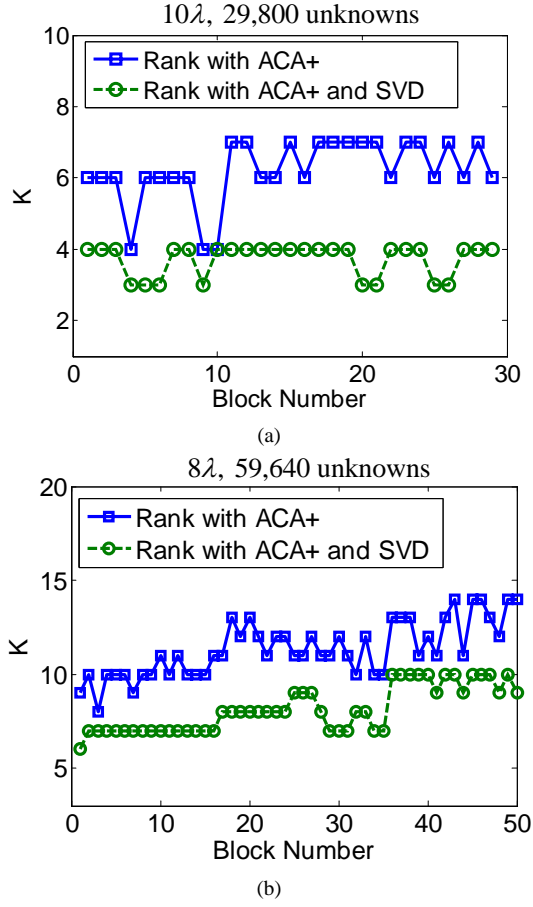


Fig. 6. Rank distribution in the lowest level of an \mathcal{H} -partition generated with $\epsilon = 10^{-4}$. (a) A 10λ perfect electrically conducting (PEC) plate. (b) An 8λ PEC sphere.

simulated a 3D conducting plate of 10 wavelengths, and a 3D conducting sphere of 8 wavelengths respectively. The ϵ in ACA+ and SVD was set to be 10^{-4} . In Fig. 6, we plot the rank distributions with the proposed scheme (ACA+ and SVD) and with ACA+ only in the lowest \mathcal{H} -partition level that has an admissible block. This level is the closest to the root of a block cluster tree, and hence the admissible blocks therein have the largest electric size. The horizontal axis of Fig. 6 is the admissible block index. It can be seen from Fig. 6 that by using the proposed method, the rank in most admissible blocks is reduced by half. Moreover, the same accuracy is achieved. The accuracy is measured by $\|\mathbf{G} - \tilde{\mathbf{G}}\| / \|\mathbf{G}\|$, where a Frobenius norm is used. The accuracy is 1.021689×10^{-5} without the proposed rank minimization, and 1.079537×10^{-5} with the proposed minimization for the plate example. Clearly, the rank is reduced without sacrificing accuracy. The same is true for the sphere example. The accuracy is 1.931219×10^{-5} without the proposed rank minimization, and 1.996355×10^{-5} with the proposed minimization. In addition, with the proposed method, the new rank distribution becomes more uniform across all the admissible blocks as can be seen from Fig. 6.

B. Proposed method for optimizing \mathcal{H} -matrix partition to reduce $k_{ave}C_{sp}$

Existing \mathcal{H} -matrix partition is based on the admissibility condition as shown in (5). It is not an optimal one for frequency dependent kernels. This can also be understood from the fact that the admissibility condition (5) is frequency independent. Physically speaking, whether the interaction between two regions can be represented by a low-rank block or not is frequency dependent. For example, for a given accuracy, it is possible that an off-diagonal block that is inadmissible at certain frequency becomes admissible at a lower frequency. It is also possible that multiple small admissible blocks can be merged into a single admissible block with prescribed accuracy. In other words, they start to become admissible in a lower level of an inverted block cluster tree when frequency changes. However, the admissibility condition given in (5) is empirical instead of theoretical. It is controlled by an empirical parameter η , instead of a prescribed accuracy.

In the following, we show our proposed algorithm that can optimize an \mathcal{H} -matrix partition based on a prescribed accuracy. The resultant \mathcal{H} -matrix partition is frequency dependent. It significantly reduces the number of admissible blocks at each tree level, with the prescribed accuracy satisfied.

The proposed \mathcal{H} -matrix partition algorithm for a prescribed accuracy ϵ_{opt} is shown in (17). A new error tolerance ϵ_{opt} is introduced instead of reusing ϵ in (16) to facilitate separated accuracy control of the \mathcal{H} -partition optimization and the rank minimization for each admissible block. In (17), the original partition given by (5) is used as an initial guess from which we construct an optimized partition.

\mathcal{H} -Partition Optimization

Procedure $\mathcal{H} - \mathcal{P}_{opt}(\mathcal{P}, \epsilon_{opt})$

```

(Input  $\mathcal{P}$  is the original  $\mathcal{H}$  partition,
output  $\mathcal{P}$  is overwritten by an optimized  $\mathcal{H}$  partition)
If  $\mathcal{P}$  is a non-leaf off-diagonal matrix block
  for ( $i = 0; i < 4; i++$ )
    if  $\mathcal{P}(i)$  is an inadmissible block
      Rk_Factor( $\mathcal{P}(i), \epsilon_{opt}$ )
    end if
    if  $\mathcal{P}(i)$  is a non-leaf block
       $\mathcal{H} - \mathcal{P}_{opt}(\mathcal{P}(i), \epsilon_{opt})$ 
    end if
  end for
If all blocks in  $\mathcal{P}$  are admissible blocks
  Merge_Rkblocks( $\mathcal{P}, \epsilon_{opt}$ )
end if
end if
  
```

(17)

In (17), the function **Rk_Factor** is to factorize a full-matrix block to a rank- k matrix shown in (6) based on a prescribed accuracy. The procedure is the combined ACA+

with SVD, which is detailed in section IV-A. The function **Merge_Rkblocks** is to merge multiple small admissible blocks to a single one based on the prescribed accuracy. To give an example, four admissible sub-blocks can be merged into one admissible block as follows.

$$\begin{aligned} & \begin{bmatrix} \mathbf{A}_1(f_1)\mathbf{B}_1(f_1)^T & \mathbf{A}_2(f_2)\mathbf{B}_2(f_2)^T \\ \mathbf{A}_3(f_3)\mathbf{B}_3(f_3)^T & \mathbf{A}_4(f_4)\mathbf{B}_4(f_4)^T \end{bmatrix} = \\ & \begin{bmatrix} \mathbf{A}_1(f_1) \\ 0 \end{bmatrix} \begin{bmatrix} \mathbf{B}_1(f_1) \\ 0 \end{bmatrix}^T + \begin{bmatrix} \mathbf{A}_2(f_2) \\ 0 \end{bmatrix} \begin{bmatrix} 0 \\ \mathbf{B}_2(f_2) \end{bmatrix}^T + \\ & \begin{bmatrix} 0 \\ \mathbf{A}_3(f_3) \end{bmatrix} \begin{bmatrix} \mathbf{B}_3(f_3) \\ 0 \end{bmatrix}^T + \begin{bmatrix} 0 \\ \mathbf{A}_4(f_4) \end{bmatrix} \begin{bmatrix} 0 \\ \mathbf{B}_4(f_4) \end{bmatrix}^T = \\ & \tilde{\mathbf{A}}_1(f_1)\tilde{\mathbf{B}}_1(f_1)^T + \tilde{\mathbf{A}}_2(f_2)\tilde{\mathbf{B}}_2(f_2)^T + \tilde{\mathbf{A}}_3(f_3)\tilde{\mathbf{B}}_3(f_3)^T + \\ & \tilde{\mathbf{A}}_4(f_4)\tilde{\mathbf{B}}_4(f_4)^T \stackrel{\epsilon_{opt}}{=} \mathbf{AB}^T, \end{aligned} \quad (18)$$

where the $f_i (i = 1, 2, 3, 4)$ denotes the electric size the blocks are associated with, and the addition in the final step is carried out by the truncated addition operation in ([17], p. 110), with the new rank k determined based on the accuracy requirement ϵ_{opt} . Different from static problems, in electrodynamic problems, when the size of the admissible block increases, its rank also increases in general. Consequently, although each merging operation reduces four admissible blocks to one block, it also increases the rank of the resultant block. Therefore, we should check which one is computationally more efficient: merging or not merging. This can be assessed by comparing the storage requirement of the merged block with that of the four children admissible blocks. If the former is less than the latter, we perform merging; otherwise, we do not perform merging, instead we keep the original four blocks. To be more specific, we check whether $k_{merge}(m_{merge} + n_{merge}) \leq \sum_{j=1}^4 k_j(m_j + n_j)$ is satisfied or not, where k_{merge} is the rank of the big block resulting from the merging operation, $m_{merge}(n_{merge})$ is the row(column) dimension of the block, and k_j is the rank of the children admissible blocks. If it is satisfied, we merge blocks based on accuracy requirements; if not, we keep the original blocks.

In (17), we only perform two basic operations: making an inadmissible block in the off-diagonal part admissible based on a prescribed accuracy via function **Rk_Factor**, or merging small admissible blocks to be a big admissible block based on the accuracy requirement through function **Merge_Rkblocks**. Both operations do not increase the number of inadmissible blocks. In fact, the number of inadmissible blocks is even reduced due to the first operation. Therefore, given an \mathcal{H} -partition, the proposed optimization algorithm does not increase the number of inadmissible blocks. If the number of admissible blocks is reduced, the total number of blocks is also reduced.

To validate the effectiveness of the proposed \mathcal{H} -partition optimization algorithm, we simulated a conducting plate from 2λ to 60λ , the number of unknowns of which is from 1,160 to 1,078,800. The ϵ_{opt} was chosen as 10^{-3} . In Fig. 7, we plot the maximum number of admissible blocks that can be formed by one cluster in a block cluster tree (C_{ad}) in the original \mathcal{H} -partition, and that in the optimized \mathcal{H} -partition. Clearly, the C_{ad} is reduced significantly. Since the proposed \mathcal{H} -partition

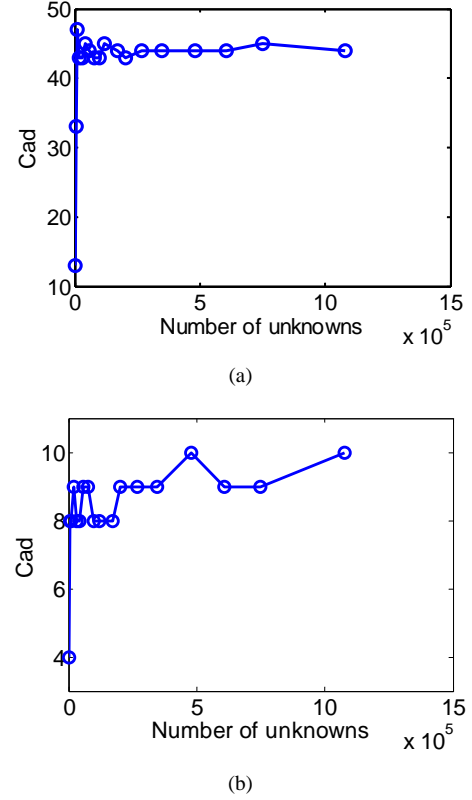


Fig. 7. C_{ad} versus N in the simulation of a conducting plate from 2λ to 60λ . (a) Original \mathcal{H} -partition. (b) Optimized \mathcal{H} -partition.

optimization does not increase the number of inadmissible blocks as analyzed above, the C_{sp} is also reduced significantly.

When the \mathcal{H} -partition changes, the average *partition* rank k_{ave} also changes. Thus, in addition to C_{sp} , we need to examine the product of k_{ave} and C_{sp} to assess the success of the proposed \mathcal{H} -partition optimization algorithm, since it is $k_{ave}C_{sp}$ that determines the storage and time complexity as can be seen from (12) and (15). In Fig. 8(a), we plot $k_{ave}C_{ad}$ for the plate example simulated above with respect to κa , where κ is the wave number, and a is the side length of the plate. We compare the $k_{ave}C_{ad}$ generated by the proposed method, and that generated by the conventional method that is based on an ACA-based rank scheme and an admissibility condition based \mathcal{H} -partition. It is clear that the proposed method greatly reduces $k_{ave}C_{ad}$. In Fig. 8(b), we plot $k_{ave}C_{ad}$ for a sphere of diameter a with respect to κa from 2λ to 45λ . Again, $k_{ave}C_{ad}$ is greatly reduced by the proposed method. Since the proposed \mathcal{H} -partition optimization does not increase the number of inadmissible blocks as analyzed above, the $k_{ave}C_{sp}$ is also reduced significantly.

Although C_{sp} is a parameter that can be used to qualitatively measure the number of blocks formed by an \mathcal{H} -partition, it does not give a *quantitative* measurement of the number of blocks obtained by the \mathcal{H} -partition. To provide a quantitative analysis, in Fig. 9(a), we plot the exact number of blocks with respect to tree level generated by the original \mathcal{H} -partition that is based on the admissibility condition in comparison with

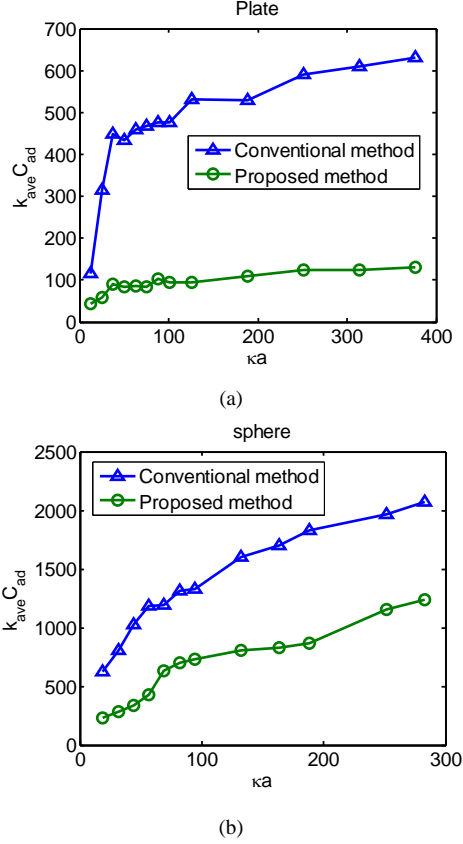


Fig. 8. Comparison between $k_{ave} C_{sp}$ generated by conventional method and that generated by the proposed method. (a) A PEC plate from 2λ to 60λ . (b) A sphere from 2λ to 45λ .

the number of blocks generated by the proposed partition, for a 15λ sphere. In Fig. 9(b), we plot the same for a 40λ plate. Clearly, compared to the original partition, the proposed partition significantly reduces the number of blocks at each tree level, and hence significantly reducing the computational cost. In addition, across the entire tree depth, it is observed that the number of blocks is not necessarily reduced by half when one ascends the inverted tree by one level from leaf level $l = p$ to root level $l = 0$, which can be seen from both conventional partition and the proposed partition.

C. Study on the dependence of k_{ave} and C_{sp} of the proposed methods with respect to scatterer shape

We varied the scattering shape continuously from plate, Sierpinski gasket, cylinder, open cone, cone sphere, to sphere. We plotted the maximal rank k_{max} versus electric size for these scatterers. For comparison, we also plotted the average partition rank k_{ave} obtained by the proposed methods for the same accuracy. As can be seen from the figures in the left column of Fig. 10 and Fig. 11, for all these scatterers, k_{ave} is much smaller compared to k_{max} . In addition, the rate of the change of k_{ave} with respect to electric size is much slower than that of k_{max} . Denoting the electric size by a/λ , where a is the maximal size of the structure, k_{max} is observed to be $O(a/\lambda)$. However, k_{ave} is not, it is much smaller than $O(a/\lambda)$. Theoretically speaking, this is because k_{ave} is not

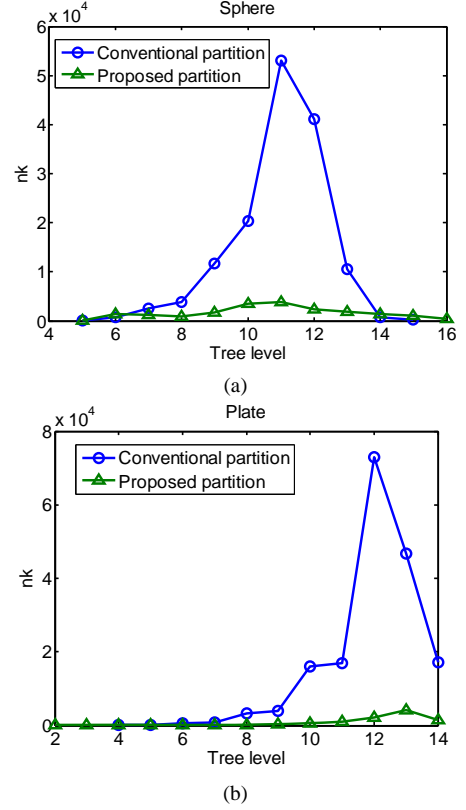


Fig. 9. Comparison between the number of blocks generated by the conventional geometry-based partition and that by the proposed optimal partition with respect to tree level. (a) A 15λ sphere. (b) A 40λ sphere.

only determined by the rank of each admissible block, but also determined by the number of admissible blocks at each tree level, and hence the \mathcal{H} -partition. In addition, compared to k_{max} , k_{ave} is less shape dependent.

In the right column of Fig. 10 and Fig. 11, we plot the number of admissible blocks obtained by the proposed method with respect to electric size for a variety of scatter shapes. The dependence of the C_{sp} on the scatter shape is shown to be little. In addition, with proposed methods, both k_{ave} and C_{sp} are minimized to be small compared to N .

D. Study on the dependence of k_{ave} and C_{sp} on accuracy requirements

We also tested the dependence of k_{ave} and C_{sp} with respect to accuracy. The results in Fig. 10 and Fig. 11 were generated based on $\epsilon = 10^{-4}$ and $\epsilon_{opt} = 10^{-3}$, where ϵ is a parameter shown in (16) for controlling the accuracy of rank reduction, and ϵ_{opt} is a parameter shown in (17) for controlling the accuracy of the \mathcal{H} -partition optimization. To test the dependence with respect to accuracy, we set $\epsilon = 10^{-7}$ and $\epsilon_{opt} = 10^{-6}$. We used a plate and a sphere as examples, and tested the dependence of k_{ave} and C_{sp} generated by the proposed methods with respect to accuracy across a wide range of electric sizes. As can be seen from Fig. 12, with the accuracy requirement increased, k_{ave} and $\sqrt{(k^2)_{ave}}$ increase. However, the increase is small compared to the three orders of magnitude increase in accuracy. In

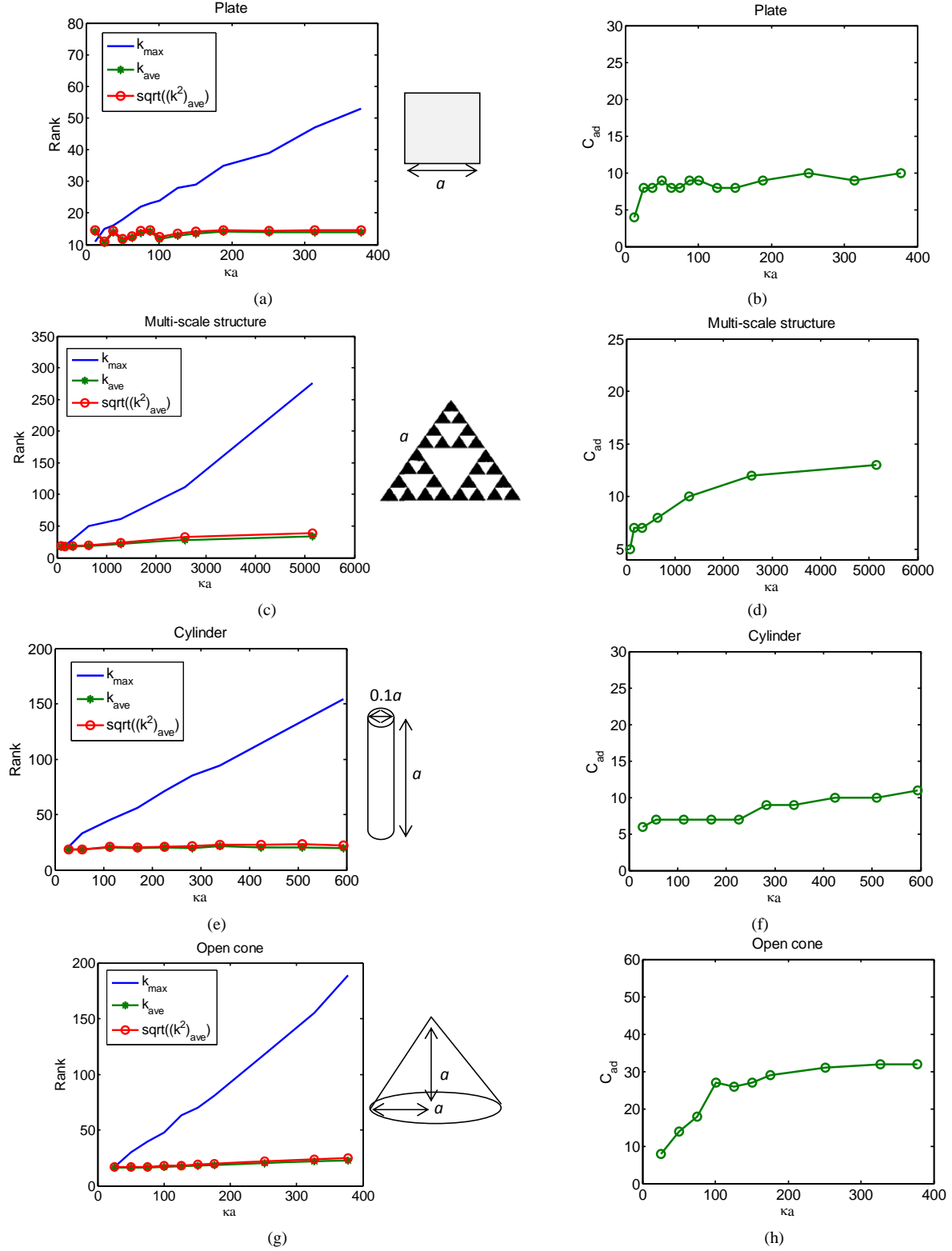


Fig. 10. The k_{ave} and C_{sp} generated by the proposed method with respect to electric size for a variety of scatterer shapes. (a-b) Plate. (c-d) Sierpinski gasket. (e-f) Cylinder. (g-h) Open cone.

addition, the dependence of k_{ave} and $\sqrt{(k^2)_{\text{ave}}}$ with respect to electric size is similar to what is observed for a lower order of accuracy. In addition, with the accuracy requirement increased, the number of admissible blocks also increases. Again, the increase is minor compared to the three orders of magnitude

increase in accuracy. Moreover, the frequency dependence of C_{sp} is also similar to that for a lower order of accuracy.

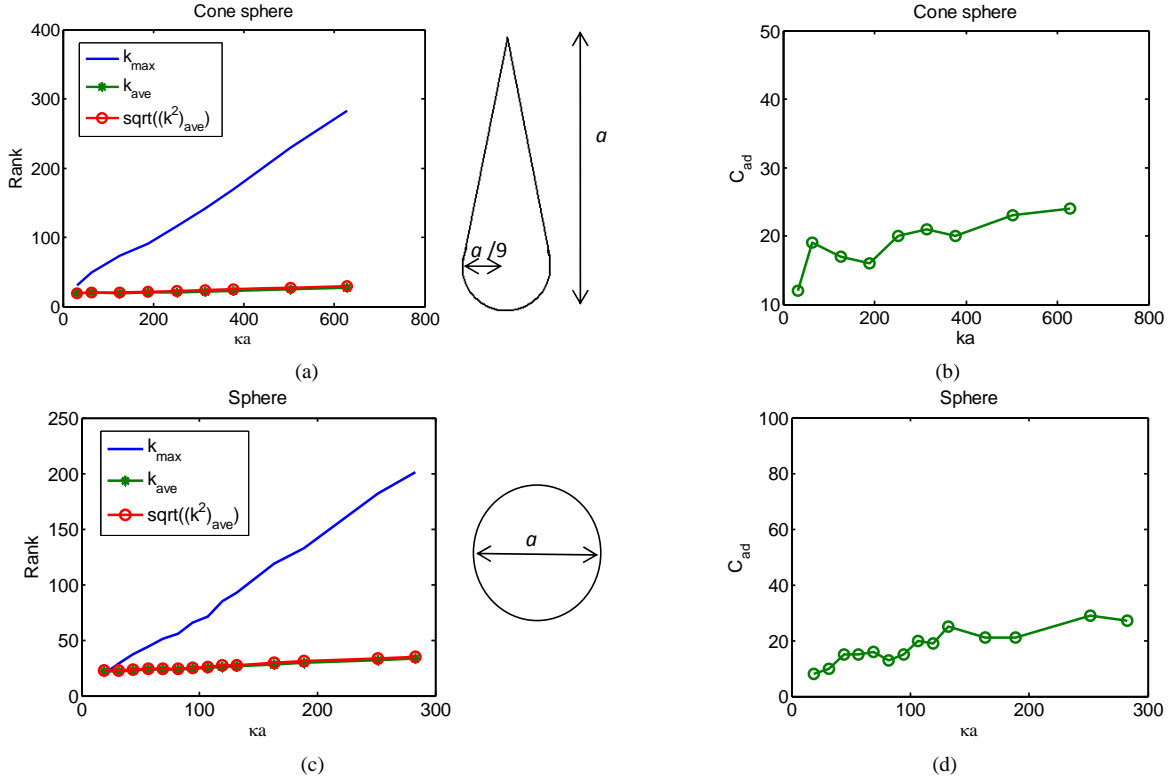


Fig. 11. The k_{ave} and C_{sp} generated by the proposed method with respect to electric size for a variety of scatterer shapes (Continued from Fig. 10). (a-b) Cone sphere. (c-d) Sphere.

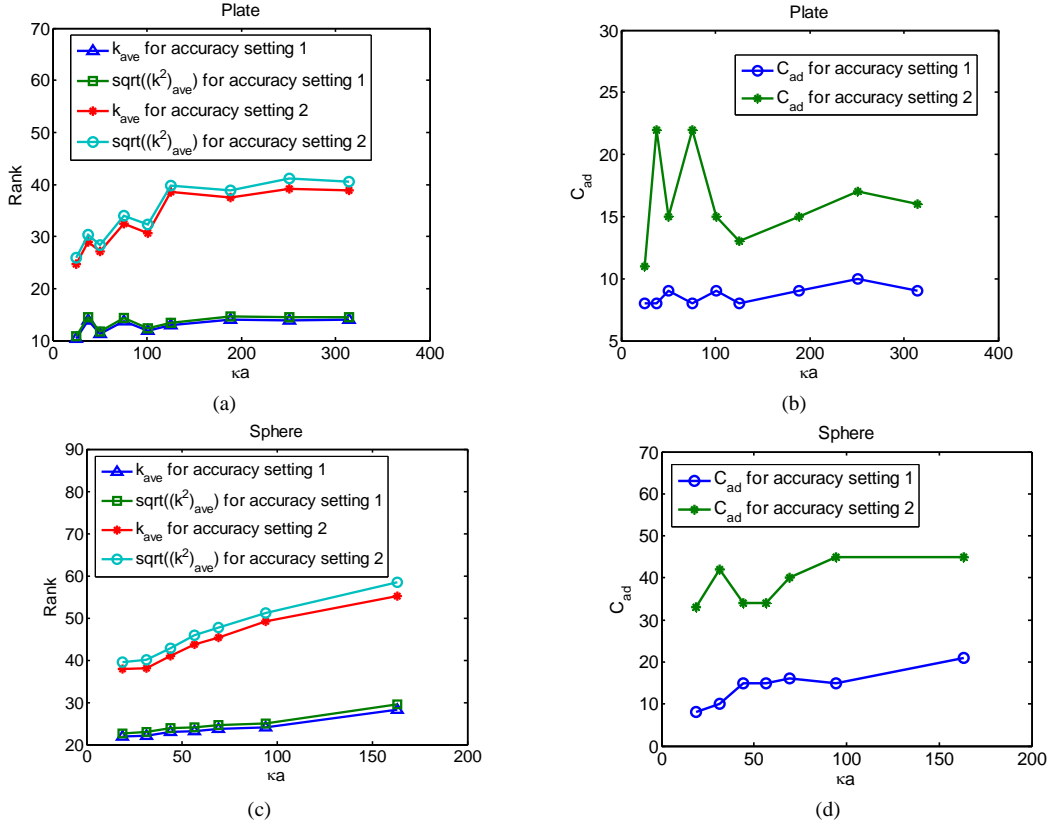


Fig. 12. The dependence of k_{ave} and C_{sp} generated by the proposed method with respect to accuracy requirements over a wide range of electric sizes (Accuracy setting 1: $\epsilon = 10^{-4}$ and $\epsilon_{\text{opt}} = 10^{-3}$; Accuracy setting 2: $\epsilon = 10^{-7}$ and $\epsilon_{\text{opt}} = 10^{-6}$). (a-b) Plate. (c-d) Sphere.

V. ON THE EXISTENCE OF THE \mathcal{H} -MATRIX REPRESENTATION OF \mathbf{G}^{-1} AND \mathbf{G} 's LU FACTORS

In this section, we numerically prove the existence of an \mathcal{H} -matrix representation of the inverse of \mathbf{G} and \mathbf{G} 's LU factors by examining their rank distributions. The detailed procedure is as follows: we directly compute \mathbf{G}^{-1} and \mathbf{G} 's LU factors without introducing any approximation; we then use SVD to obtain the rank distribution in \mathbf{G}^{-1} and \mathbf{G} 's LU factors. Since the computation requires a complete full-matrix form of \mathbf{G}^{-1} and \mathbf{G} 's LU factors, it is not practical to use a problem having a large electric size as an example. We thus considered a conducting plate of 6λ and a conducting sphere of 4λ . We computed the rank of each off-diagonal block that satisfies the admissibility condition (5) at the lowest level of a block cluster tree. The accuracy requirement in SVD is set to be 10^{-4} . In Fig. 13, we plot the rank distribution measured by $k/\min(m, n)$ with respect to matrix block index. It is clear that the off-diagonal blocks that satisfy the admissibility condition in \mathbf{G}^{-1} and \mathbf{G} 's LU factors are low rank. Therefore, not only the original matrix \mathbf{G} can be represented by an \mathcal{H} -matrix, but also \mathbf{G}^{-1} and \mathbf{G} 's LU factors can be represented by an \mathcal{H} -matrix. Furthermore, the rank distribution of \mathbf{G}^{-1} and \mathbf{G} 's LU factors is very similar to that of \mathbf{G} . In addition, both \mathbf{G}^{-1} and \mathbf{G} 's LU factors have a smaller rank than the original matrix, with the rank of \mathbf{G} 's LU factors being the smallest. This suggests that the \mathcal{H} -matrix partition constructed for the original matrix \mathbf{G} is equally applicable to \mathbf{G}^{-1} and \mathbf{G} 's LU factors. In Fig. 13, \mathbf{U} 's rank distribution is plotted to represent \mathbf{L} 's and \mathbf{U} 's rank distribution since these two have a very similar rank distribution, with \mathbf{U} 's rank being slightly larger.

VI. PROPOSED FAST IMPLEMENTATION OF LU FACTORIZATION

In this section, we show how to perform a fast LU factorization using the \mathcal{H} -matrix based representation of \mathbf{G} and \mathbf{G} 's LU factors. Based on the findings in the section above, we use the \mathcal{H} -partition constructed for \mathbf{G} for the \mathcal{H} -partition of \mathbf{L} and \mathbf{U} .

The \mathcal{H} -based LU factorization has been discussed in ([17], p. 119). However, no detailed implementation is given. In the following, we give a number of pseudo-codes to show a fast implementation of \mathcal{H} -based LU factorization, which is not reported anywhere else. It is worth mentioning that [10] did an ACA-based LU factorization, the procedure of which is very different from the proposed one. The fast \mathcal{H} -based LU factorization proposed in this paper has a factorization cost of $O((k_{ave}C_{sp})^2N \log^2 N)$, a solution cost of $O((k_{ave}C_{sp})N \log N)$, and memory consumption of $O((k_{ave}C_{sp})N \log N)$, with k_{ave} and C_{sp} minimized for a prescribed accuracy by the methods described in section IV.

A. LU factorization basics

Given an IE-based system matrix \mathbf{G} , we cast it into a form

$$\mathbf{G} = \begin{bmatrix} \mathbf{G}_{11} & \mathbf{G}_{12} \\ \mathbf{G}_{21} & \mathbf{G}_{22} \end{bmatrix}. \quad (19)$$

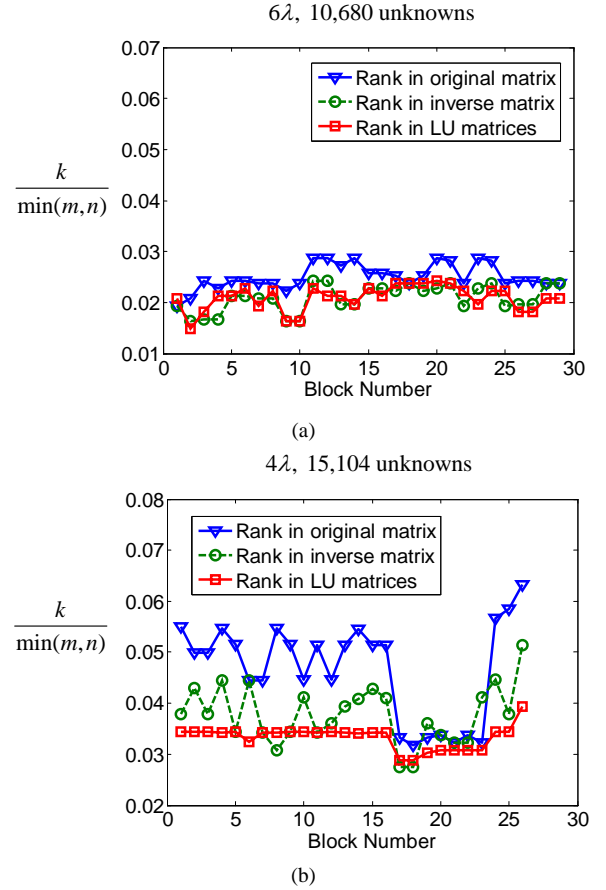


Fig. 13. Rank distributions in \mathbf{G} , \mathbf{G}^{-1} , and \mathbf{G} 's LU factors. (a) PEC plate. (b) PEC sphere.

The LU decomposition can be recursively computed by the following equation:

$$\mathbf{G} = \begin{bmatrix} \mathbf{G}_{11} & \mathbf{G}_{12} \\ \mathbf{G}_{21} & \mathbf{G}_{22} \end{bmatrix} = \begin{bmatrix} \mathbf{L}_{11} & 0 \\ \mathbf{L}_{21} & \mathbf{L}_{22} \end{bmatrix} \cdot \begin{bmatrix} \mathbf{U}_{11} & \mathbf{U}_{12} \\ 0 & \mathbf{U}_{22} \end{bmatrix} = \mathbf{LU}. \quad (20)$$

B. Proposed fast implementation of the LU factorization

We developed a pseudo-code shown in (21) to recursively perform LU factorization.

LU-Decomposition $\mathbf{G}=\mathbf{LU}$

Procedure \mathcal{H} -LU(\mathbf{G})

(\mathbf{G} is the input matrix overwritten by \mathbf{L} and \mathbf{U})

If \mathbf{G} is a non-leaf block

\mathcal{H} -LU(\mathbf{G}_{11}) $\rightarrow \mathbf{L}_{11}, \mathbf{U}_{11}$,

Solve_LX($\mathbf{L}_{11}, \mathbf{G}_{12}$) $\rightarrow \mathbf{U}_{12}$,

Solve_XU($\mathbf{G}_{21}, \mathbf{U}_{11}$) $\rightarrow \mathbf{L}_{21}$,

$-\mathbf{L}_{21} \times \mathbf{U}_{12} + \mathbf{G}_{22} \rightarrow \mathbf{G}_{22}$,

\mathcal{H} -LU(\mathbf{G}_{22}) $\rightarrow \mathbf{L}_{22}, \mathbf{U}_{22}$,

else

Full-LU(\mathbf{G})

(21)

The underlying algorithm is as follows. When \mathbf{G} is a non-leaf matrix block, we recursively call (21) until \mathbf{G}_{11} is a full matrix block. We then directly compute the LU factors of the \mathbf{G}_{11} using a full-matrix-based LU factorization, which generates \mathbf{L}_{11} and \mathbf{U}_{11} . Next, we call function **Solve_LX** shown in (22) and **Solve_XU** to compute \mathbf{U}_{12} , and \mathbf{L}_{21} respectively.

Algorithm for Solving a Lower Triangular System

$\mathbf{LX} = \mathbf{G}$, with \mathbf{G} being an \mathcal{H} matrix

Procedure **Solve_LX**(\mathbf{L}, \mathbf{G})

```

  ( $\mathbf{L}$  and  $\mathbf{G}$  are input matrices,  $\mathbf{G}$  is overwritten by  $\mathbf{X}$ )
  If  $\mathbf{L}$  is a non-leaf block
    If  $\mathbf{G}$  is a non-leaf block
      Solve_LX( $\mathbf{L}_{11}, \mathbf{G}_{11}$ ), Solve_LX( $\mathbf{L}_{11}, \mathbf{G}_{12}$ )
       $-\mathbf{L}_{21} \times \mathbf{G}_{11} + \mathbf{G}_{21} \rightarrow \mathbf{G}_{21}$ , Solve_LX( $\mathbf{L}_{22}, \mathbf{G}_{21}$ )
       $-\mathbf{L}_{21} \times \mathbf{G}_{12} + \mathbf{G}_{22} \rightarrow \mathbf{G}_{22}$ , Solve_LX( $\mathbf{L}_{22}, \mathbf{G}_{22}$ )
    else if  $\mathbf{G}$  is an admissible block
      Solve_LF( $\mathbf{L}, \mathbf{A}$ )
    else
      Solve_LF( $\mathbf{L}, \mathbf{G}$ )
  end if
else
  Full_LX( $\mathbf{L}, \mathbf{G}$ )
  (Solve a full-matrix triangular system)
end if

```

(22)

The **Solve_LX**(\mathbf{L}, \mathbf{G}) is to solve a lower triangular system $\mathbf{LX} = \mathbf{G}$, where \mathbf{L} and \mathbf{G} are input matrices having \mathcal{H} -representations, and \mathbf{X} is the solution. The **Solve_XU**(\mathbf{G}, \mathbf{U}) is to solve an upper triangular system, which can be derived in a similar fashion as (22). In (22), a function **Solve_LF** is called. Similar to **Solve_LX**, **Solve_LF** also solves a triangular system. The difference is that the right-hand-side matrix for **Solve_LX** is an \mathcal{H} matrix, whereas that for **Solve_LF** is a full matrix. The pseudo-code of **Solve_LF** is given in (23).

Algorithm for Solving a Lower Triangular System

$\mathbf{LX} = \mathbf{F}$, with \mathbf{F} being a Full Matrix

Procedure **Solve_LF**(\mathbf{L}, \mathbf{F})

```

  ( $\mathbf{L}$  and  $\mathbf{F}$  are input matrices,  $\mathbf{F}$  is overwritten by  $\mathbf{X}$ )
  If  $\mathbf{L}$  is a non-leaf block
    Solve_LF( $\mathbf{L}_{11}, \mathbf{F}_1$ )
     $-\mathbf{L}_{21} \times \mathbf{F}_1 + \mathbf{F}_2 \rightarrow \mathbf{F}_2$ 
    Solve_LF( $\mathbf{L}_{22}, \mathbf{F}_2$ )
  else
    Full_LX( $\mathbf{L}, \mathbf{F}$ )
  (Solve a full-matrix triangular system)

```

end if

(23)

In the final step of (21), we use \mathbf{U}_{12} and \mathbf{L}_{21} to update \mathbf{G}_{22} , and then call (21) recursively until \mathbf{L}_{22} and \mathbf{U}_{22} are computed. As can be seen from (20) to (23), efficient LU factorization relies on efficient block multiplication and block addition. In next subsection, we show how to efficiently perform these two operations for a prescribed accuracy.

C. Fast implementation of the block multiplication $\mathbf{G}^b = \mathbf{G}^{b1} \times \mathbf{G}^{b2}$

We give a pseudo-code of computing $\mathbf{G}^b = \mathbf{G}^{b1} \times \mathbf{G}^{b2}$ in (24).

Recursive Multiplication Algorithm

Procedure **H-mult**($\mathbf{G}^{b1}, \mathbf{G}^{b2}, \mathbf{G}^b, \epsilon_{LU}$)

If ($\mathbf{G}^{b1}, \mathbf{G}^{b2}, \mathbf{G}^b$ are all non-leaf blocks)

for ($i = 0; i < 2; i++$)

for ($j = 0; j < 2; j++$)

for ($k = 0; k < 2; k++$)

H-mult($\mathbf{G}^{b1}(i, k), \mathbf{G}^{b2}(k, j), \mathbf{G}^b(i, j)$)

else if (\mathbf{G}^b is a non-leaf block,

\mathbf{G}^{b1} or \mathbf{G}^{b2} is a leaf block)

Multiply_RK($\mathbf{G}^{b1}, \mathbf{G}^{b2}, \tilde{\mathbf{G}}^b$)

$\mathbf{G}^b \stackrel{\epsilon_{LU}}{=} \tilde{\mathbf{G}}^b + \mathbf{G}^b$

else if \mathbf{G}^b is an admissible block

Multiply_RK($\mathbf{G}^{b1}, \mathbf{G}^{b2}, \mathbf{G}^b$)

else if \mathbf{G}^b is an inadmissible block

Multiply_Full($\mathbf{G}^{b1}, \mathbf{G}^{b2}, \mathbf{G}^b$)

end if

(24)

where, b, b_1 , and b_2 represent three blocks in the same level of an \mathcal{H} -partition, ϵ_{LU} represents a prescribed accuracy. If $\mathbf{G}^b, \mathbf{G}^{b1}$, and \mathbf{G}^{b2} are all non-leaf blocks, we recursively call (24). If one of \mathbf{G}^{b1} and \mathbf{G}^{b2} is a leaf block, or \mathbf{G}^b is an admissible block, we call function **Multiply_Rk** shown in (25) to compute an admissible product. In (24), the addition is performed based on the prescribed accuracy ϵ_{LU} , which is denoted by $\stackrel{\epsilon_{LU}}{=}$. The detailed procedure of the addition is given in the following subsection.

Procedure **Multiply_RK**($\mathbf{G}^{b1}, \mathbf{G}^{b2}, \mathbf{G}^b, \epsilon_{LU}$)

if \mathbf{G}^{b1} and \mathbf{G}^{b2} are both non-leaf blocks

for ($i = 0; i < 2; i++$)

for ($j = 0; j < 2; j++$)

for ($k = 0; k < 2; k++$)

Multiply_RK($\mathbf{G}^{b1}(i, k), \mathbf{G}^{b2}(k, j), \tilde{\mathbf{G}}^b(i, j)$)

$\mathbf{G}^b \stackrel{\epsilon_{LU}}{=} \tilde{\mathbf{G}}^b + \mathbf{G}^b$

($\tilde{\mathbf{G}}^b$ is a non-leaf block)

else if \mathbf{G}^{b1} or \mathbf{G}^{b2} is an admissible block
 $\mathbf{G}^{b1}\mathbf{A}\mathbf{B}^T \rightarrow (\mathbf{G}^{b1}\mathbf{A})\mathbf{B}^T = \tilde{\mathbf{A}}_b\tilde{\mathbf{B}}^T = \tilde{\mathbf{G}}^b$
 ($\tilde{\mathbf{G}}^b$ is an admissible block)
 $\mathbf{G}^b \stackrel{\epsilon_{LU}}{=} \tilde{\mathbf{G}}^b + \mathbf{G}^b$
 else if \mathbf{G}^{b1} or \mathbf{G}^{b2} is an inadmissible block
 $\mathbf{G}^{b1}\mathbf{G}^{b2} = \mathbf{G}^{b1}\mathbf{F} \stackrel{\epsilon_{LU}}{\rightarrow} (\mathbf{G}^{b1}\mathbf{A})\mathbf{B}^T = \tilde{\mathbf{A}}_b\tilde{\mathbf{B}}^T = \tilde{\mathbf{G}}^b$
 $\mathbf{G}^b \stackrel{\epsilon_{LU}}{=} \tilde{\mathbf{G}}^b + \mathbf{G}^b$
 end if

(25)

In (25), there are two multiplication cases. One is to multiply an admissible block \mathbf{G}^{b1} by an admissible block of an $\mathbf{A}\mathbf{B}^T$ form, for which we can compute $\mathbf{G}^{b1}\mathbf{A}$ as a new \mathbf{A} . The other multiplication case is to multiply \mathbf{G}^{b1} by a full matrix block \mathbf{F} , for which we can first apply SVD to \mathbf{F} to generate a form $\mathbf{A}\mathbf{B}^T$ based on the prescribed accuracy ϵ_{LU} . If \mathbf{G}^b is a full matrix block, a normal full matrix multiplication is computed. The additions in (25) again are performed based on ϵ_{LU} .

D. Fast implementation of the block addition $\mathbf{G}^b = \mathbf{G}^{b1} + \mathbf{G}^{b2}$

Two cases are involved in the addition operations.

Case 1: If \mathbf{G}^b , \mathbf{G}^{b1} , and \mathbf{G}^{b2} have the same \mathcal{H} -partition, the addition can be done using the following procedure. (a) If three blocks are all full matrices, we simply add two full matrices up. (b) If three blocks are all admissible matrices, for example, $\mathbf{G}^{b1} = \mathbf{A}_{b1}\mathbf{B}_{b1}^T$ with rank k_1 , $\mathbf{G}^{b2} = \mathbf{A}_{b2}\mathbf{B}_{b2}^T$ with rank k_2 , and $\mathbf{G}^b = \mathbf{A}_b\mathbf{A}_b^T$, the $\mathbf{G}^b = \mathbf{G}^{b1} + \mathbf{G}^{b2}$ can be realized by a truncated addition operation using the approach shown in ([17], p. 110). The rank k of the resultant \mathbf{G}^b is adaptively determined by the prescribed accuracy ϵ_{LU} . (c) If three blocks are all non-leaf blocks, the addition can be carried out by summing over all the inadmissible blocks using (a), and all the admissible ones using (b) respectively.

Case 2: If the three blocks do not share the same partition, we convert the \mathcal{H} -matrix partitions of \mathbf{G}^{b1} and \mathbf{G}^{b2} both into the partition of \mathbf{G}^b . Take the block \mathbf{G}^{b1} as an example. If \mathbf{G}^{b1} is an admissible block but \mathbf{G}^b is a non-leaf block that has four admissible subblocks, we convert \mathbf{G}^{b1} by the following formula

$$\begin{aligned}
 \mathbf{G}^{b1} &= \\
 \mathbf{A}_{b1}\mathbf{B}_{b1}^T &= \begin{bmatrix} \tilde{\mathbf{A}}_1 \\ \tilde{\mathbf{A}}_2 \end{bmatrix} \begin{bmatrix} \tilde{\mathbf{B}}_1 \\ \tilde{\mathbf{B}}_2 \end{bmatrix}^T = \\
 &\begin{bmatrix} \tilde{\mathbf{A}}_1\tilde{\mathbf{B}}_1^T & \tilde{\mathbf{A}}_1\tilde{\mathbf{B}}_2^T \\ \tilde{\mathbf{A}}_2\tilde{\mathbf{B}}_1^T & \tilde{\mathbf{A}}_2\tilde{\mathbf{B}}_2^T \end{bmatrix} = \tilde{\mathbf{G}}^{b1}.
 \end{aligned} \tag{26}$$

where $\tilde{\mathbf{G}}^{b1}$ contains four admissible sub-blocks, which is exactly equal to \mathbf{G}^{b1} . The opposite procedure, where \mathbf{G}^b is an admissible block while \mathbf{G}^{b1} contains four admissible sub-blocks, can be performed by the scheme shown in (18).

VII. COMPLEXITY ANALYSIS

Three numerical procedures are involved in the proposed direct IE solver: rank minimization, \mathcal{H} -partition optimization, and LU-based direct matrix solution. We analyze the complexity of each in the following.

The complexity of the rank minimization scheme for each admissible block, described in section IV-A, is linear. This is because both ACA+ and reduced SVD have a linear complexity for each admissible block [17], [20].

For the \mathcal{H} -partition optimization shown in (17), two basic operations are involved. One is the factorization of inadmissible blocks. This operation is carried out by the function **Rk_Factor** based on ACA+ and SVD. The other is the conversion of non-leaf blocks into an admissible block shown in (18). This operation is carried out by the function **Merge_Rkblocks** by using an SVD based truncated addition. Since both ACA+ and SVD have a linear complexity for each matrix block, the two basic operations involved in (17) also have a linear cost.

From procedure (21), it can be seen that at the leaf level, the computation of the recursive LU factorization essentially includes a full-matrix LU factorization, a full-matrix solution of a lower triangular system, and a full-matrix solution of an upper triangular system, all of which have the same complexity as a full-matrix block multiplication. At all the other levels, a number of block-block multiplications are computed, which have the same recursive pattern as that in an \mathcal{H} -based matrix-matrix multiplication. Therefore, the \mathcal{H} -based LU factorization has the same complexity as \mathcal{H} -based multiplication, which is bounded by $O((k_{ave}C_{sp})^2 N \log^2 N)$ for electrodynamic problems as derived in (15). The \mathcal{H} -based LU solution has the same complexity as the \mathcal{H} -based matrix-vector multiplication, and hence its cost is $O((k_{ave}C_{sp})N \log N)$ for electrodynamic problems as derived in (12). Here, $k_{ave}C_{sp}$ is minimized for a given accuracy by the methods proposed in section IV.

VIII. NUMERICAL RESULTS

To test the performance of the proposed direct IE solver, we simulated a PEC (perfect electrically conducting) plate, a PEC sphere, and a PEC cylinder from a small number of unknowns to over 1 million unknowns, from small electric sizes to over 95 wavelengths. In all these examples, $\eta = 1$ and $leafsize = 32$ were used. Note that $\eta = 1$ was used to generate an initial \mathcal{H} -partition, which was later replaced by the optimized \mathcal{H} -partition by the method proposed in Section IV-B. The error tolerance ϵ_{opt} used in the \mathcal{H} -partition optimization was set as 10^{-3} . The error tolerance ϵ_{LU} used in the LU factorization was 10^{-2} . The computer used was a Dell's PowerEdge 6950s server with 8222SE AMD Opteron processors. Double precision was employed in all the simulations.

First, we tested the accuracy of the \mathcal{H} -matrix representation obtained by the proposed rank minimization and partition optimization methods. The error of the \mathcal{H} -matrix representation is measured by $\|\mathbf{G} - \tilde{\mathbf{G}}\| / \|\mathbf{G}\|$, where $\tilde{\mathbf{G}}$ is the \mathcal{H} -matrix representation of the original \mathbf{G} , and the Frobenius norm is used. We simulated a PEC plate from 2λ to 14λ , and a PEC sphere from 2λ to 8λ . Fig. 14 shows the accuracy of the \mathcal{H} -matrix representation generated from the proposed method.

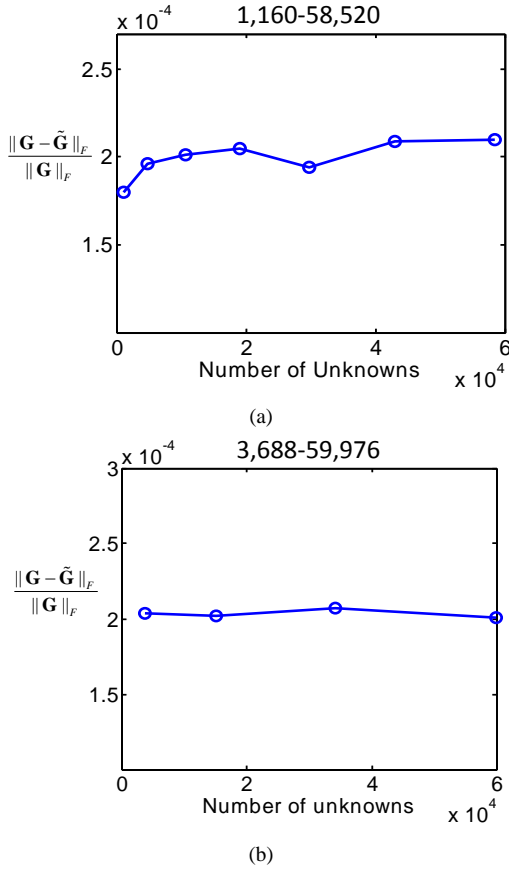


Fig. 14. Accuracy of the proposed \mathcal{H} -matrix representation. (a) PEC plate from 2λ to 14λ . (b) PEC sphere from 2λ to 8λ .

Excellent accuracy can be observed in the entire range of electric sizes. Since the assessment of the matrix error requires the knowledge of the full matrix \mathbf{G} , we did not simulate larger problem sizes in this testing case.

Next, we tested the accuracy and efficiency of the proposed direct LU based IE solver. The first example is a conducting sphere illuminated by a normally incident plane wave. The electric size of the sphere is from 2λ to 45λ . The discretization results in unknowns from 3,688 to 1,152,368. The average partition rank k_{ave} resulting from the proposed rank minimization and \mathcal{H} -partition optimization methods is shown in Fig. 15(a) in the entire range of electric sizes. It can be seen that k_{ave} is minimized to be a small number compared to N . In Fig. 15(b), we plot the memory cost of the proposed solver. The theoretical expectation is also plotted for comparison, which is shown by the red solid line. Excellent agreement with the theoretical analysis is observed. In 15(c) and (d), we plot the CPU time of the LU decomposition, and LU solution respectively. Again, an excellent agreement with the theoretical prediction is observed. To test the accuracy, in Fig. 16(a) and (b), we plot the E-plane bi-static RCS simulated for 12λ and 26λ respectively. The RCS is shown to agree well with the analytical Mie-Series solution. In Fig. 16(c), we plot the solution error. Less than 6% error is observed in the entire frequency band.

The second example is a 3D conducting plate, the electric size of which is from 2λ to 60λ . The discretization results in

1,160 unknowns to 1,078,800 unknowns. The average partition rank k_{ave} resulting from the proposed rank minimization and partition optimization methods is shown in Fig. 17(a). It is clear that the average rank is minimized to be a small number, in addition, for the plate example, it is controlled to be almost a constant in the entire range of electric sizes. The C_{sp} for this example can be seen from Fig. 7(b). In Fig. 17(b), we plot the memory cost of the proposed direct IE solver, which agrees well with the theoretical prediction depicted by the solid line. In Fig. 17(c), we plot the solution error of the proposed LU solver measured by $\|\tilde{\mathbf{G}}\mathbf{I} - \mathbf{V}\| / \|\mathbf{V}\|$. Good accuracy can be observed. In addition, the accuracy is kept to be almost a constant in the entire range. From Fig. 17(d) to (f), we plot the CPU time of the \mathcal{H} -matrix construction, LU decomposition, and LU solution respectively. It can be seen clearly that the computational cost of the proposed direct LU solver has a very good agreement with the theoretical prediction depicted by the solid lines. The computation for the 60λ case having over 1 million unknowns was finished within 10-hour LU decomposition time, 55-second LU solution time, and costing 31.5 GB storage only.

The last example is a conducting cylinder, the length of which is from 2λ to 96λ . The ratio of length to radius is 20. The number of unknowns is from 1,391 to 1,075,200. In Fig. 18(a), we plot the average partition rank k_{ave} resulting from the proposed rank minimization and partition optimization methods in the entire electric-size range. In Fig. 18(b), we plot C_{ad} versus the electric size. Without the proposed \mathcal{H} -partition optimization, the C_{ad} is between 47 and 51. Clearly, C_{ad} , and hence C_{sp} is reduced greatly. In Fig. 19(a), we plot the solution error with respect to the number of unknowns. Good accuracy is observed. Note that the error is controllable by ϵ , ϵ_{opt} , and ϵ_{LU} . If better accuracy is required, it can be obtained by reducing the error tolerances. From Fig. 19(b) to (d), we show the computational cost of the proposed direct LU solver in LU factorization, LU Solution, and storage. Again, an excellent agreement with theoretical analysis is observed. The LU factorization for the 1,075,200 unknown case costs less than 20 hours and 37.6 GB memory. The LU solution time is 85 seconds only. Compared to results obtained for similar examples reported in open literature, the proposed direct IE solver is much more efficient in both CPU time and memory consumption, even though double precision was used for computation.

The above direct matrix solutions were all generated based on $\epsilon = 10^{-4}$, $\epsilon_{opt} = 10^{-3}$, and $\epsilon_{LU} = 10^{-2}$. To test the performance of the proposed direct solver for a higher order of accuracy, we set $\epsilon = 10^{-5}$, $\epsilon_{opt} = 10^{-4}$, and $\epsilon_{LU} = 10^{-3}$. We simulated the same plate example simulated in Fig. 17. In Fig. 20(a), we plot the solution error with respect to the number of unknowns. An excellent accuracy can be observed in the entire range of electric sizes, where the worst error is shown to be less than 0.33%, in comparison with the 3% error achieved by the previous accuracy setting. From Fig. 20(b) to (d), we show the computational cost of the proposed direct LU solver in memory, LU factorization, and LU solution. Again, an excellent agreement with theoretical analysis is observed.

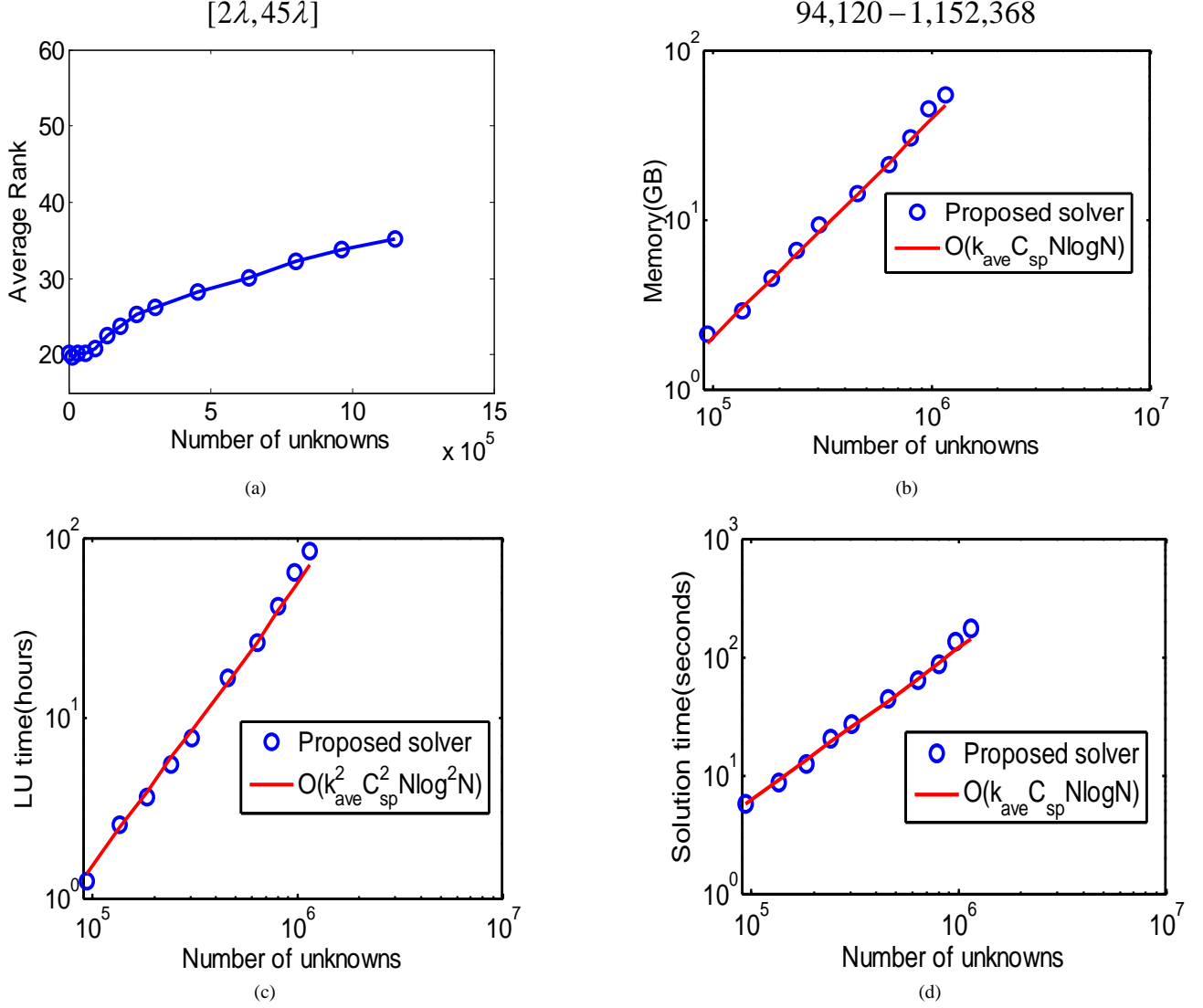


Fig. 15. Simulation of a PEC sphere from 2λ to 45λ with unknowns from 3,688 to 1,152,368. (a) Average partition rank k_{ave} . (b) Memory requirement. (c) LU factorization time. (d) LU solution time.

IX. CONCLUSION

In this work, we further develop the \mathcal{H} -matrix based mathematical framework to accelerate the direct solution of the integral-equation-based analysis of electrodynamic problems. We show that the existing complexity analysis of the \mathcal{H} -matrix based computation, which is based on a constant rank, is not proper for analyzing electrodynamic problems. This is because the rank of each block required by an electrodynamic kernel for a given accuracy increases with the electric size of the block diameter. It is not a constant any more. However, using the maximal rank of all the admissible blocks to bound the complexity also overestimates the complexity, as demonstrated clearly in Fig. 4. In addition, the complexity of an \mathcal{H} -matrix based computation of electrodynamic problems is highly dependent on the \mathcal{H} -matrix partition, i.e. the number of admissible blocks at each tree level and etc. This is an important factor that received little attention in previous research. Traditionally, the number of admissible blocks at tree level l is treated as $O(2^l)$, and the rank of each admissible

block at tree level l is regarded as $O(\frac{N}{2^l})$. As a result, the gain in computational efficiency of an \mathcal{H} -matrix based method for solving high-frequency problems is pessimistic.

In this work, we show that there exists a big space to optimize the \mathcal{H} -matrix partition for frequency dependent problems. Existing \mathcal{H} -matrix partition is based on a geometry based admissibility condition. This condition is controlled by an empirical parameter instead of a prescribed accuracy. The resultant partition is by no means optimal especially for electrodynamic problems. We hence develop a new \mathcal{H} -partition method that is frequency dependent, and also directly controlled by accuracy requirements. With the proposed new partition, the number of admissible blocks at each tree level is significantly reduced compared to that generated by the conventional geometry based \mathcal{H} -partition. We also show that the number of admissible blocks at tree level l is *not* $O(2^l)$.

In addition, the block rank is observed to be proportional to the electric size of the block diameter, as can be seen from Fig. 10 and Fig. 11. Since the number of unknowns in a surface

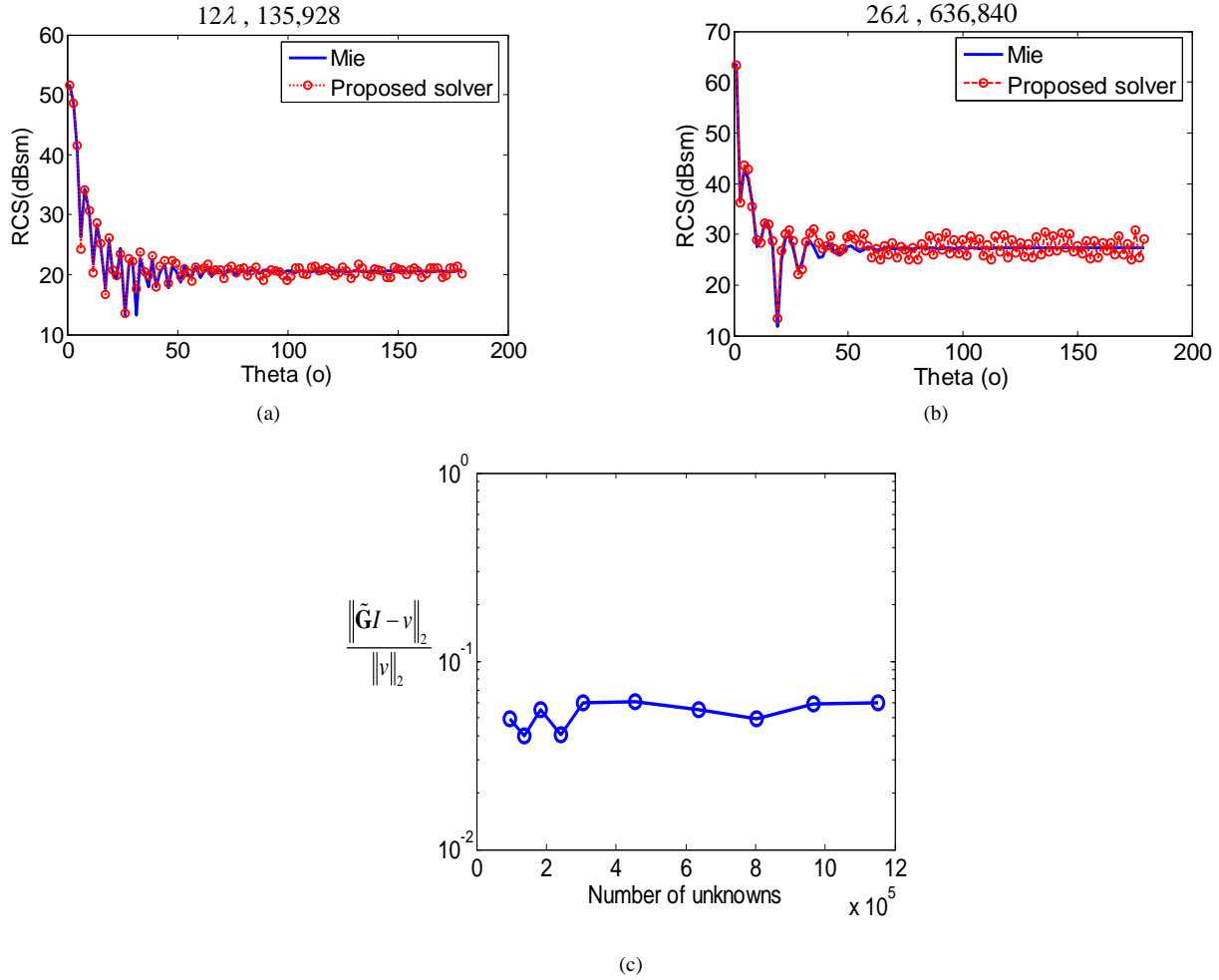


Fig. 16. (a) RCS of a conducting sphere simulated by the proposed solver at 12 λ . (b) RCS of a conducting sphere simulated by the proposed solver at 26 λ . (c) Solution error in the entire frequency band from 2 λ to 45 λ .

IE based method is proportional to the electric size's square, the rank of each admissible block at tree level l is bounded by $O((\frac{N}{2^l})^{0.5})$ instead of $O(\frac{N}{2^l})$, thus the block is low rank. In addition, the actual number of the block rank should be determined and minimized based on accuracy requirements. This paper provides an efficient matrix algebra based method to perform this task with negligible computational overhead.

In light of the fact that the complexity of an \mathcal{H} -matrix based computation of electrodynamic problems is determined not only by block rank (the rank of each admissible block) but also by \mathcal{H} -matrix partition, we propose a new parameter, average partition rank k_{ave} , to bound the storage units and operation counts of an \mathcal{H} -matrix based computation. Different from block rank, the partition rank k_{ave} contains the information of the \mathcal{H} -matrix partition. Based on k_{ave} , we develop new bounds of the computational cost for the \mathcal{H} -matrix-based computation of electrodynamic problems. The new bounds suggest that the smaller the product $k_{ave}C_{sp}$ is, the smaller the computational cost. For electrodynamic problems, the k_{ave} and C_{sp} are frequency dependent and hence electric size dependent. The objective of this work is to minimize the $k_{ave}C_{sp}$ for each frequency point to reduce computational cost. The k_{ave} for a given partition is minimized by finding a minimal rank of each

admissible block for a given accuracy. The C_{sp} and $k_{ave}C_{sp}$ are reduced by developing a new \mathcal{H} -partition algorithm. By minimizing $k_{ave}C_{sp}$ for each frequency point, we significantly reduce the cost of the \mathcal{H} -matrix based direct solution of electrodynamic problems.

Moreover, we developed an efficient LU-factorization for directly solving the dense system matrix resulting from an IE-based analysis of large-scale electrodynamic problems. The operation counts of the proposed direct solver are $O((k_{ave}C_{sp})^2 N \log^2 N)$ in LU factorization, $O((k_{ave}C_{sp})N \log N)$ in LU solution, and the memory consumption is $O(k_{ave}C_{sp}N \log N)$, all of which were verified theoretically and also numerically. Numerical results have demonstrated the accuracy and efficiency of the proposed direct IE solver for simulating large-scale electrodynamic problems, with the N -dependent k_{ave} and C_{sp} minimized to be small compared to N . The dense matrix involving over 1 million unknowns formulated for a 96-wavelength problem is factorized in fast CPU run time, modest memory usage, and with prescribed accuracy satisfied. The proposed methods for minimizing the rank and optimizing the \mathcal{H} -partition not only can be used in the proposed solver, but also can be employed in other fast integral equation solvers such as fast multipole

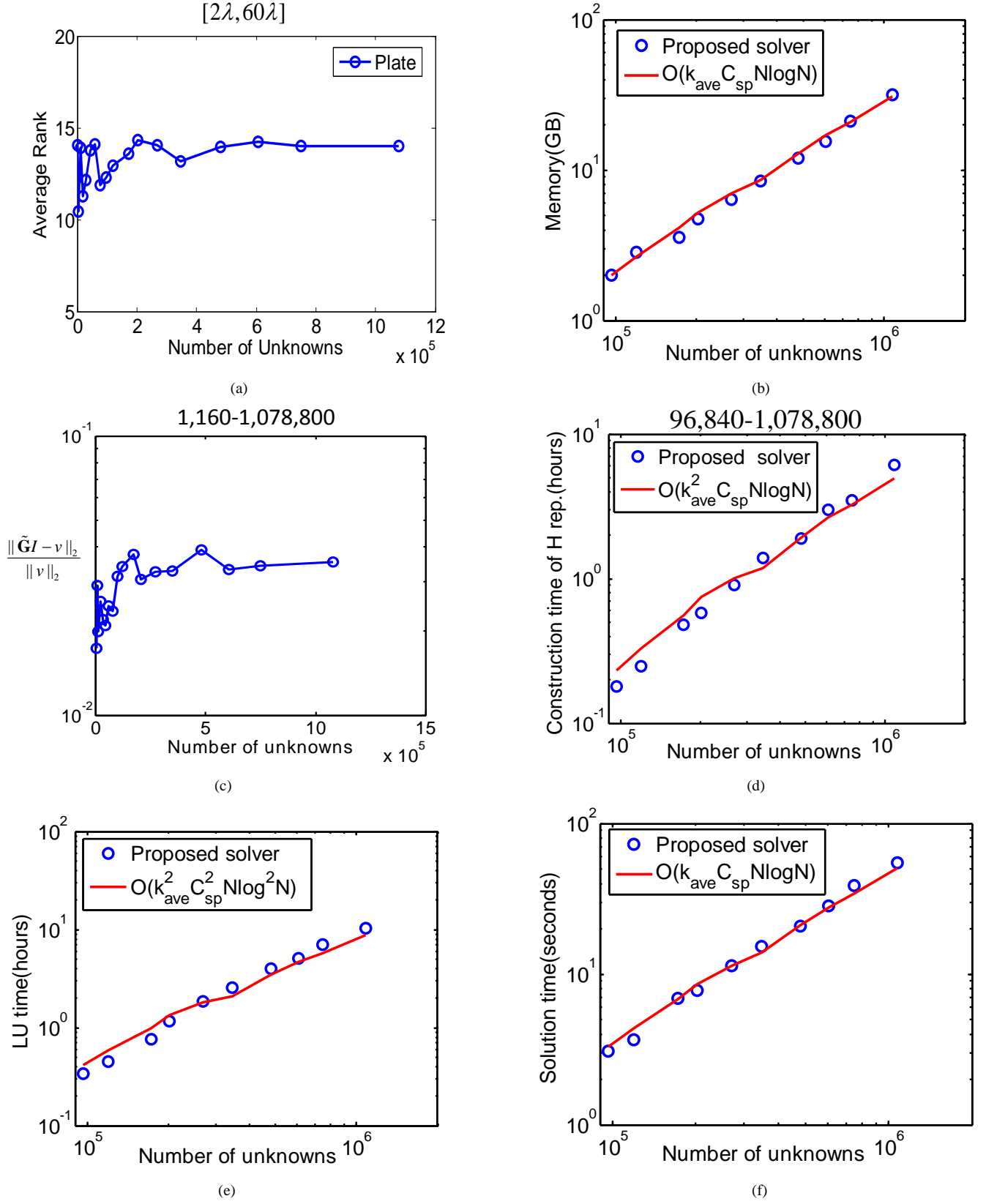


Fig. 17. Simulation of a PEC plate from 2λ to 60λ . (a) Average partition rank. (b) Memory cost. (c) Solution error. (d) \mathcal{H} -matrix construction time. (e) LU factorization time. (f) LU solution time.

based methods.

REFERENCES

- [1] W. Chew, J. Jin, E. Michielssen, and J. Song, *Fast and Efficient Algorithms in Computational Electromagnetics*. Norwood, MA: Artech

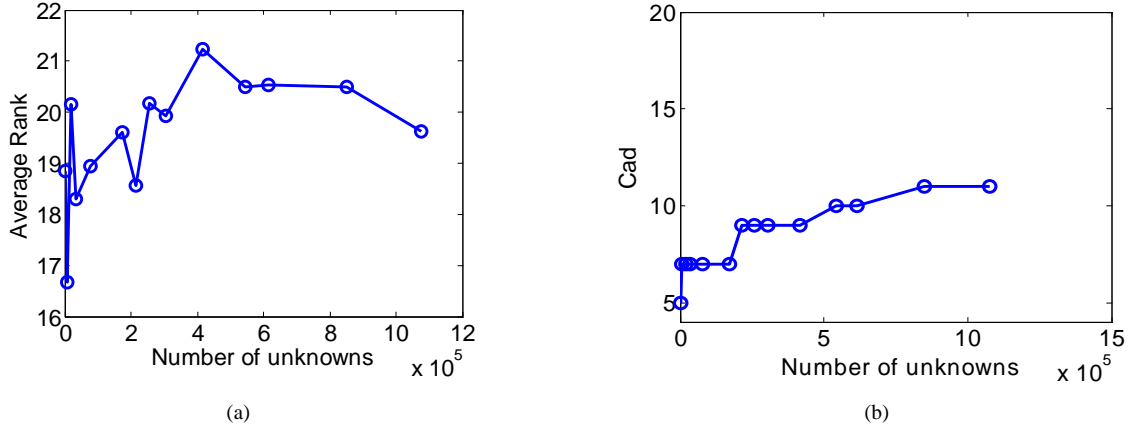


Fig. 18. Simulation of a PEC cylinder from 2λ to 96λ . (a) k_{ave} versus N . (b) C_{ad} versus N .

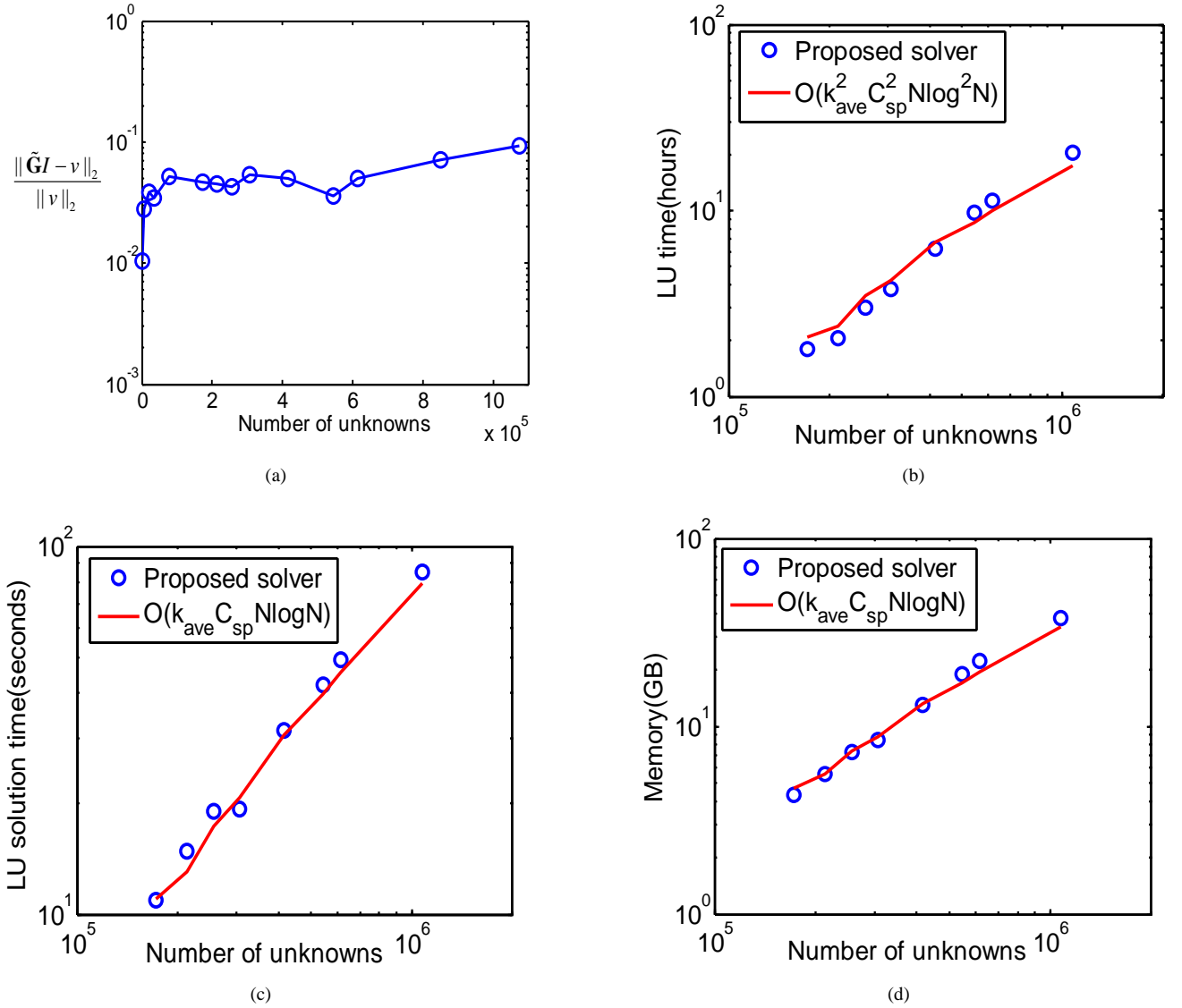


Fig. 19. Simulation of a PEC cylinder from 2λ to 96λ . (a) Solution error. (b) LU factorization time. (c) LU solution time. (d) Memory Cost.

House, 2001.

- [2] V. Rokhlin, "Rapid solution of integral equations of scattering in two dimensions," *J. Comput. Phys.*, vol. 86, pp. 419–439, Feb 1990.
- [3] J. Song, C. Lu, and W. Chew, "Multilevel fast multipole algorithm

for electromagnetic scattering by large complex objects," *IEEE Trans. Antennas Propag.*, vol. 45, no. 10, pp. 1488–1493, Oct 1997.

- [4] S. Kapur and D. E. Long, "IES3: A fast integral equation solver for efficient 3-dimensional extraction," *IEEE/ACM Int. Conf. Comput.-Aided*

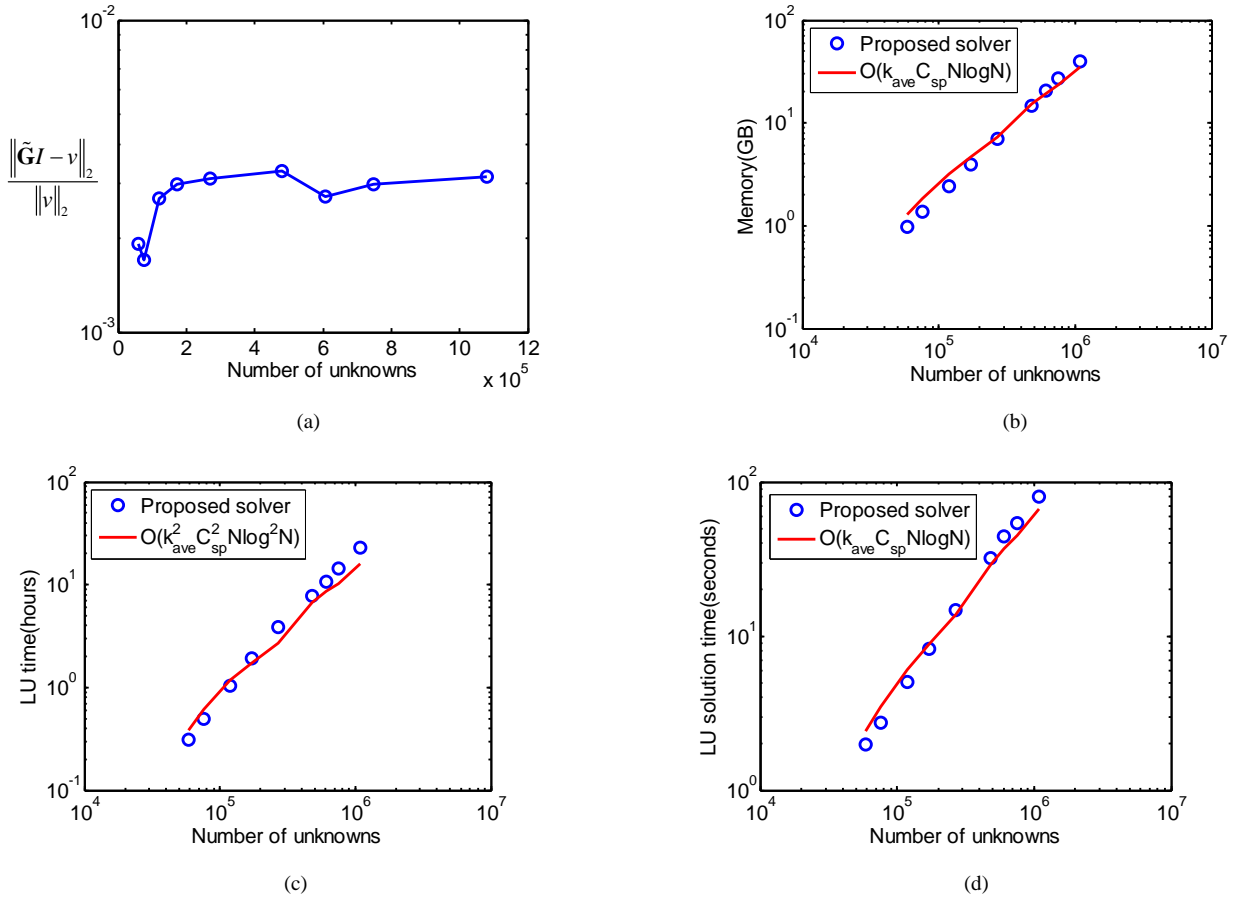


Fig. 20. Simulation of a PEC plate from 2λ to 60λ based on a higher-order accuracy setting ($\epsilon = 10^{-5}$, $\epsilon_{opt} = 10^{-4}$, and $\epsilon_{LU} = 10^{-3}$). (a) Solution error. (b) Memory Cost. (c) LU factorization time. (d) LU solution time.

- Design Dig.*, pp. 448–455, Nov 1997.
- [5] M. Seo and J. F. Lee, "A single-level low rank IE-QR algorithm for PEC scattering problems using EFIE formulation," *IEEE Trans. Antennas Propag.*, vol. 52, no. 8, pp. 2141–2146, Aug 2004.
 - [6] R. J. Burkholder and J. F. Lee, "Fast dual-MGS block-factorization algorithm for dense MoM matrices," *IEEE Trans. Antennas Propag.*, vol. 52, no. 7, pp. 1693–1699, July 2004.
 - [7] D. Gope and V. Jandhyala, "Efficient solution of EFIE via low-rank compression of multilevel predetermined interactions," *IEEE Trans. Antennas Propag.*, vol. 53, no. 10, pp. 3324–3333, Oct. 2005.
 - [8] N. N. Bojarski, "k-space formulation of the electromagnetic scattering problem," *Tech. Rep. AFAL-TR-71-75*, Air Force Avionics Lab., March 1971.
 - [9] E. Bleszynski, M. Bleszynski, and T. Jarozewicz, "AIM: Adaptive integral method for solving large-scale electromagnetic scattering and radiation problems," *Radio Sci.*, vol. 31, no. 10, pp. 1225–1251, Sept.-Oct. 1996.
 - [10] J. Shaeffer, "Direct Solve of Electrically Large Integral Equations for Problem Sizes to 1 M unknowns," *IEEE Trans. Antennas Propag.*, vol. 56, no. 8, pp. 2306–2313, Aug. 2008.
 - [11] R. J. Adams, Y. Xu, X. Xu, S. D. Gedney, and F. X. Canning, "Modular Fast Direct Electromagnetic Analysis Using Local-Global Solution Modes," *IEEE Trans. Antennas Propag.*, vol. 56, no. 8, pp. 2427–2441, Aug. 2008.
 - [12] W. Chai and D. Jiao, "An \mathcal{H}^2 -Matrix-Based Integral-Equation Solver of Reduced Complexity and Controlled Accuracy for Solving Electrodynamical Problems," *IEEE Trans. Antennas Propag.*, vol. 57, no. 10, pp. 3147–3159, Oct. 2009.
 - [13] W. Chai and D. Jiao, " \mathcal{H} and \mathcal{H}^2 -Matrix-Based Fast Integral-Equation Solvers for Large-Scale Electromagnetic Analysis," *IET Microwaves, Antennas and Propagation*, accepted for publication, 2009.
 - [14] W. Hackbusch and B. Khoromskij, "A sparse matrix arithmetic based on H-matrices. Part I: Introduction to \mathcal{H} -matrices," *Computing*, vol. 62, pp. 89–108, 1999.
 - [15] W. Hackbusch and B. Khoromskij, "A sparse matrix arithmetic. Part II: Application to multi-dimensional problems," *Computing*, vol. 64, pp. 21–47, 2000.
 - [16] S. Borm, "Introduction to hierarchical matrices with applications," *EABE*, vol. 27, pp. 403–564, 2003.
 - [17] S. Borm, L. Grasedyck, and W. Hackbusch, "Hierarchical matrices," *Lecture note 21 of the Max Planck Institute for Mathematics in the Sciences*, 2003.
 - [18] W. Chai, D. Jiao, and C. Koh, "A Direct Integral-Equation Solver of Linear Complexity for Large-Scale 3D Capacitance and Impedance Extraction," *46th ACM/EDAC/IEEE Design Automation Conference*, pp. 752–757, July 2009.
 - [19] W. Hackbusch, B. Khoromskij, and S. Sauter, "On \mathcal{H}^2 -matrices," *Lecture on Applied Mathematics*, H. Bungartz, R. Hoppe, and C. Zenger, eds., pp. 9–29, 2000.
 - [20] M. Bebendorf, "Approximation of boundary element matrices," *Numer. Math.*, vol. 86, no. 4, pp. 565–589, 2000.
 - [21] K. Zhao, M. N. Vouvakis, and J. Lee, "The Adaptive Cross Approximation Algorithm for Accelerated Method of Moments Computations of EMC Problems," *IEEE Trans. EMC*, vol. 47, no. 4, pp. 763–773, 2005.
 - [22] S. M. Rao, and D. R. Wilton, "Electromagnetic scattering by surfaces of arbitrary shape," *IEEE Trans. Antennas Propag.*, vol. 30, no. 3, pp. 409–418, March 1982.